THE UNIVERSITY OF OKLAHOMA

GRADUATE COLLEGE

A GENERALIZED CORRELATION FOR PREDICTION OF FLUID THERMODYNAMIC PROPERTIES AND PHASE BEHAVIOR AND ITS INDUSTRIAL APPLICATIONS

A DISSERTATION

SUBMITTED TO THE GRADUATE FACULTY

in partial fulfillment of the requirements for the

degree of

DOCTOR OF PHILOSOPHY

BY

MOO SUP HAN

Norman, Oklahoma

1972

A GENERALIZED CORRELATION FOR PREDICTION OF FLUID THERMODYNAMIC PROPERTIES AND PHASE BEHAVIOR AND ITS INDUSTRIAL APPLICATIONS

APPROVED BY

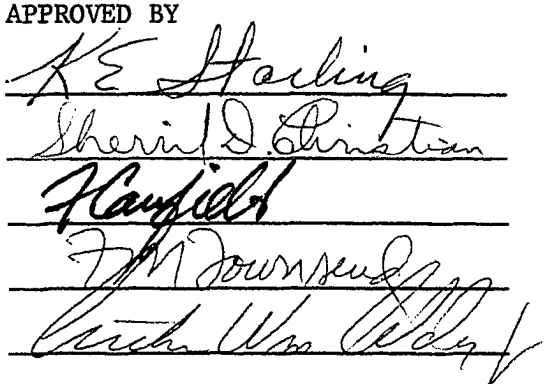

DISSERTATION COMMITTEE

ACKNOWLEDGMENTS

I would like to express my sincere gratitude and appreciation to the following persons and organizations for their part in this research:

Professor Kenneth E. Starling--for his advice, inspiration and encouragement throughout this research.

Professors Frank B. Canfield, F. Mark Townsend, James H. Christensen and Sherril D. Christian--for serving on my advisory committee.

The Department of Chemical Engineering and Materials Science--for financial support.

University of Oklahoma Computing Center--for donating computing time.

Dr. N. F. Carnahan--for his interest in the early phases of this research.

Mr. J. S. Wang, my office partner--for his friendship and the useful discussions of equation of state research.

Mrs. Ruth Kempton--for her skillfulness in typing the final manuscript.

My parents--for their patience, encouragement and love throughout my education.

My wife, Hea Ja--for her understanding, patience, personal sacrifice, encouragement and special love during my doctoral studies.

ABSTRACT

A generalized equation of state correlation has been developed for prediction of fluid thermodynamic properties and phase behavior from the effective use of recent advances in equation of state development methods. The generalized parameters in the correlation were determined using simultaneously data for the normal paraffin hydrocarbons methane through n-octane in the multiproperty regression analysis of PVT, enthalpy and vapor pressure data. Multiproperty analysis was used to ensure consistent prediction of all thermodynamic properties.

A parameter sensitivity study was made to determine the effects of each generalized parameter on saturated properties. This sensitivity study helped to provide a guide for selection of parameters which should be modified for improved prediction in a given temperature region.

The correlation makes use of an interaction parameter for binary pairs in the applications of the generalized correlation to mixtures. Values of interaction parameters determined principally from vapor-liquid equilibrium data of binary systems are tabulated.

The generalized correlation is readily adaptable to computer use. Because minimization of computing time for repetitious calculations is very important for practical use of the correlation, a new efficient density search program has been developed. The new density search program, which uses a false-position method, is faster than the Newton-Raphson method in

most regions of density and is orders of magnitude faster than the trial-and-error method.

Computational procedures for using the generalized correlation for prediction of thermodynamic behavior including fluid density, enthalpy, vapor pressure, entropy and vapor-liquid equilibrium are described.

The use of critical constraints in determining equation of state parameters is shown to improve predictions of thermodynamic behavior in the critical region, including prediction of the critical point.

Comparisons of predicted thermodynamic properties and K-values with experimental data were made for broad ranges of systems and conditions to prove the generalized correlation is capable of describing virtually all conditions encountered industrially. The pure fluids used in comparison calculations include polar and nonpolar compounds, paraffin, olefin, naphthene and aromatic hydrocarbons and nonhydrocarbons. In mixture properties comparison calculations, predicted mixture densities, enthalpies and entropies were compared with experimental or derived data for 38 mixtures at more than 1400 points. The mixtures considered include natural gas, LPG and LNG mixtures containing as many as 10 components. Phase equilibrium data for 42 systems were used to evaluate the generalized correlation for vapor-liquid equilibrium predictions.

Finally, the comparison calculations are discussed in terms of particular processing situations to emphasize the industrial applications of the correlation.

TABLE OF CONTENTS

LIST OF TABLES

LIST OF ILLUSTRATIONS

Figure Page

A GENERALIZED CORRELATION FOR PREDICTION OF FLUID THERMODYNAMIC PROPERTIES AND PHASE BEHAVIOR AND ITS INDUSTRIAL APPLICATIONS

CHAPTER I

INTRODUCTION

The objective of the research discussed in this dissertation was to develop a generalized correlation for prediction of all fluid thermodynamic properties as well as pure fluid and multicomponent phase behavior.

At the present time, the two-fluid model of corresponding states is the most accurate generalized method for predicting the bulk thermodynamic properties of nonpolar fluids [22,31,42]. The success of this method for predicting bulk properties cannot be disputed. However, for the prediction of partial molar properties and phase behavior, the two-fluid model[32], as well as other similar corresponding states methods, have met with less success than achieved in prediction of bulk properties. On the other hand, modifications[64,118] of the BWR[4] and Redlich-Kwong[89] equations have been used with considerable success recently for predictions of phase behavior. In both the corresponding states and equation of state methods, accurate prediction of partial molar properties and phase behavior requires accurate dependence of properties on composition. By either approach, composition dependence occurs through the composition dependence of the parameters which characterize the fluid, e.g., pseudocritical constants,

pseudoacentric factor, etc. in the corresponding states method, and equation parameters in the equation of state method. Although theories such as conformal solution theory in the corresponding states approach and the mixture virial equation in the equation of state approach can be used as starting points in defining composition dependence, one must ultimately resort to empirical methods for all but the simplest mixtures. Thus, the choice of methods for correlation would seem to be almost arbitrary, the corresponding states method having been generally more successful for bulk properties and the equation of state method having been generally more successful for partial molar properties and phase behavior.

The decision to use the equation of state method of correlation in the present work was based on choosing among various possibilities the combination which seemed most likely to achieve the ultimate goal of accurate prediction phase behavior as well as bulk properties.

Recent advances in equation of state development methods at University of Oklahoma include the development of the mathematical framework and computer programs for multiproperty regression analysis[21,96,97]. The most advanced multiproperty analysis can simultaneously utilize PVT, enthalpy, and vapor pressure and multicomponent vapor-liquid equilibrium data to determine optimal values of equation of state parameters[65]. The temperature and density dependence of the equation of state used in this work was developed using multiproperty analysis. This equation is capable of accurate predictions of fluid behavior at reduced temperatures as low as 0.3 and reduced densities as great as 3.2. Effective use of these recent advances in equation of state development methods has been made to develop the generalized equation of state correlation presented here.

CHAPTER II

DEVELOPMENT OF GENERALIZED EQUATION OF STATE CORRELATION

The equation of state[98] for pressure used in this work is the following function of temperature and molar density:

$$P = \rho RT + (B_o RT - A_o - \frac{C_o}{T^2} + \frac{D_o}{T^3} - \frac{E_o}{T^4}) \rho^2$$

$$+ (bRT - a - \frac{d}{T}) \rho^3 + \alpha(a + \frac{d}{T}) \rho^6 \qquad \text{(II-1)}$$

$$+ \frac{c\rho^2}{T^2} (1 + \gamma\rho^2) \exp(-\gamma\rho^2)$$

The development of Equation (II-1) has been discussed elsewhere[21,57]. The eleven parameters in Equation (II-1) have been determined individually for the normal paraffin hydrocarbons methane through n-octane as well as isobutane, isopentane, ethylene, propylene, nitrogen, carbon dioxide and hydrogen sulfide[98].

Methods for Generalization of an Equation of State

To extend the usefulness of an equation of state for which parameters have been determined only for a limited number of fluids, it is desirable

to have available a practical means for generating parameters for other fluids of interest. One simple method of generalization is to rewrite the equation of state in reduced form based on the two-parameter corresponding states principle. Su and Viswanath[104] have used this approach for the BWR equation. Pseudo-critical volume was defined in terms of critical temperature and pressure to eliminate the use of experimental critical volumes. To improve the accuracy of predictions, some investigators have expressed reduced parameters as functions of acentric factor or critical compressibility factor[28]. These generalizations based on the corresponding states principle have been applied with satisfactory results to predict the volumetric behavior of the vapor phase, but they become unreliable near the two phase region[46].

Another way to generalize an equation of state is to directly correlate equation of state parameters rather than reduced parameters, as functions of physical constants such as acentric factor, the critical constants and other characteristics of the fluids involved. For example, Canjar and co-workers[13] have correlated the BWR constants for the hydrocarbon series in terms of critical temperature and carbon number, and Starling[100] has correlated the normal paraffin BWR constants as functions of carbon number alone.

Application of the Corresponding States Principle to the Equation of State

To study the possibility of a corresponding states generalization of Equation (II-1), the corresponding relation for the compressibility factor Z was converted to the following reduced form.

$$Z = 1 + \left(B_o' - \frac{A_o'}{T_r} - \frac{C_o'}{T_r^3} + \frac{D_o'}{T_r^4} - \frac{E_o'}{T_r^5}\right)\rho_r + \left(b' - \frac{a'}{T_r} - \frac{d'}{T_r^2}\right)\rho_r^2 + \alpha'\left(\frac{a'}{T_r} + \frac{d'}{T_r^2}\right)\rho_r^5 + \frac{c'\rho_r^2}{T_r^3}\left(1 + \gamma'\rho_r^2\right)\exp\left(-\gamma'\rho_r^2\right) \qquad \text{(II-2)}$$

where

$$B_o' = B_o\rho_c \qquad \alpha' = \alpha\rho_c^3$$

$$A_o' = \frac{A_o\rho_c}{RT_c} \qquad c' = \frac{c\rho_c^2}{RT_c^3}$$

$$C_o' = \frac{C_o\rho_c}{RT_c^3} \qquad D_o' = \frac{D_o\rho_c}{RT_c^4} \qquad \text{(II-3)}$$

$$\gamma' = \gamma\rho_c^2 \qquad d' = \frac{d\rho_c^2}{RT_c^2}$$

$$b' = b\rho_c^2 \qquad E_o' = \frac{E_o\rho_c}{RT_c^5}$$

$$a' = \frac{a\rho_c^2}{RT_c}$$

Utilizing the parameters in Equation (II-1) which previously[98] had been determined individually for the eight normal paraffin hydrocarbons, the resultant reduced equation of state parameters in Equation (II-3) were plotted versus acentric factor (Figure II-1). It can be seen in Figure II-1 that the

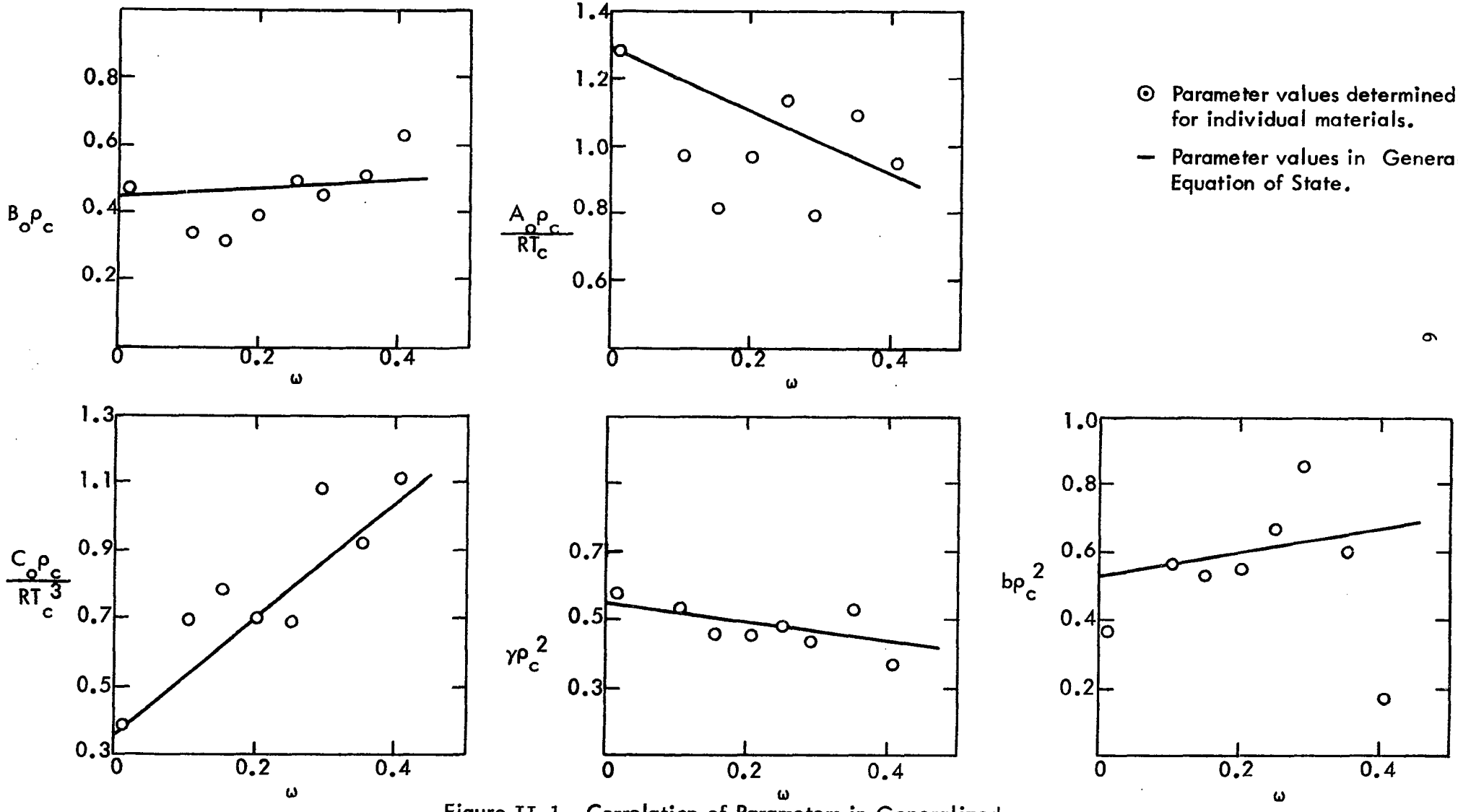

Figure II-1 Correlation of Parameters in Generalized Equation of State.

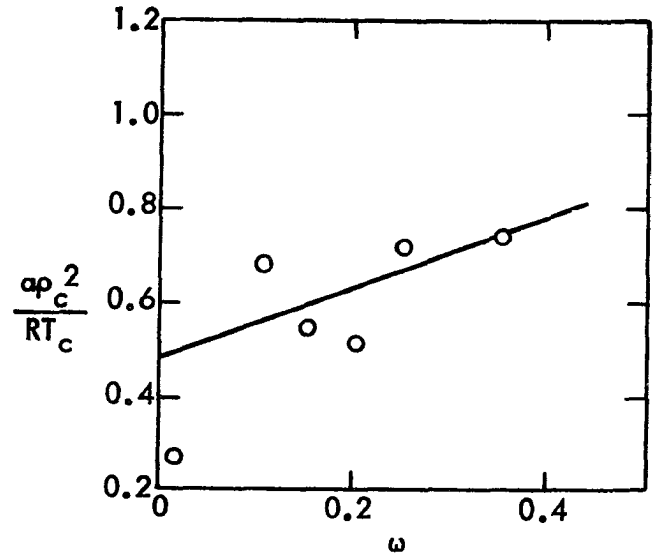

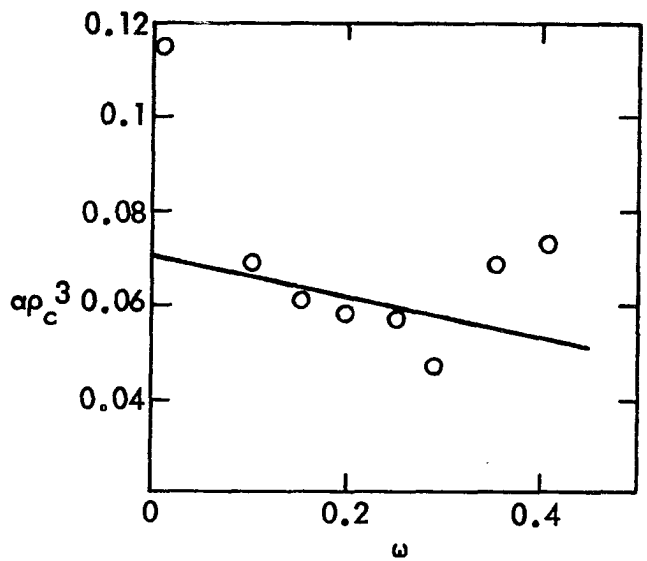

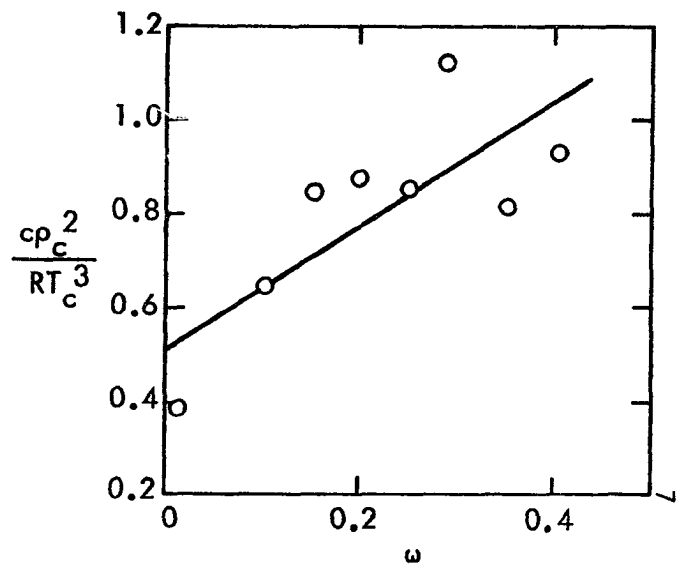

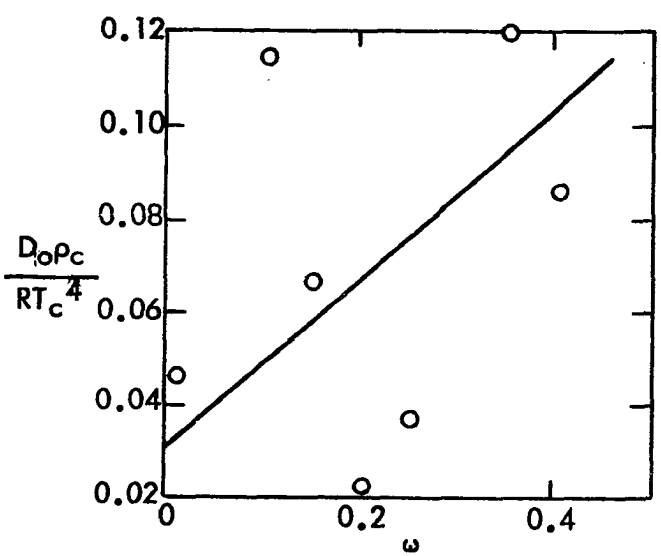

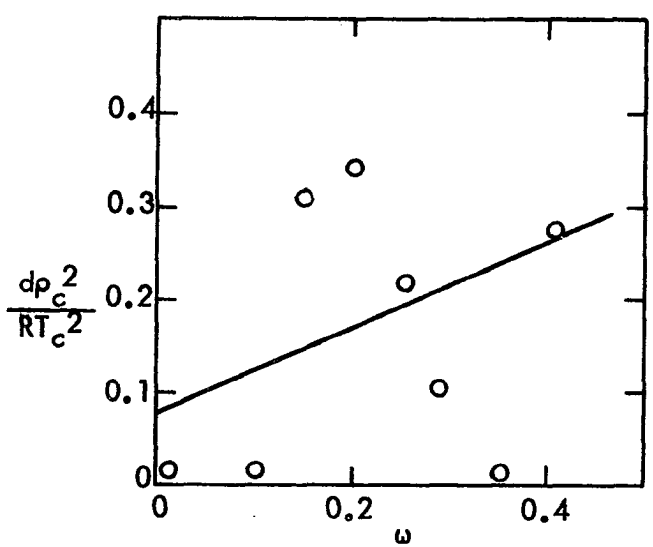

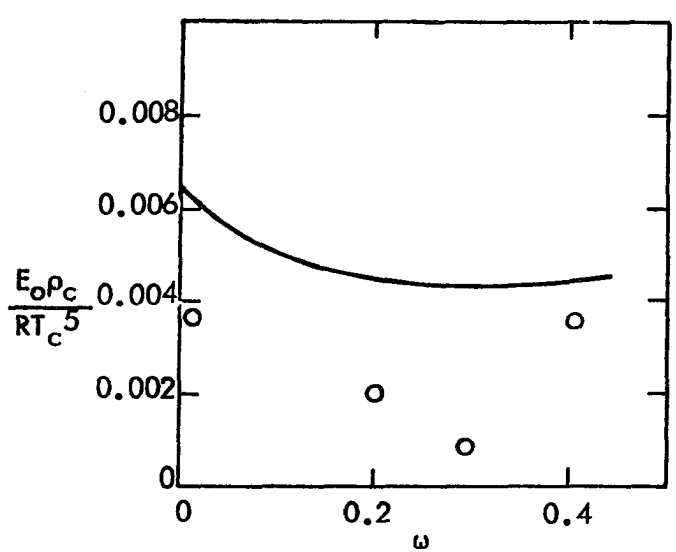

Figure II-1 (Continued)

scattering of the data points diminishes the possibility of determining from the individual component parameters the exact functionality between the reduced parameters and acentric factor. The scatter in reduced parameter values in Figure II-1 is due in part to the relatively large covariances among the eleven parameters in Equation (II-1). In a multiparameter equation of state, it is inherent that some of the parameters will have large variances, which are measures of uncertainties, and large covariances, which are measures of statistical dependence between parameter pairs. By transforming the parameters into reduced form, these uncertainties and covariance effects tend to be magnified when plotted, as in Figure II-1. This finding does not repudiate the validity of the corresponding states principle. Rather, it points out the inappropriateness of applying the corresponding states principle directly to the equation of state parameters determined for individual materials. If appropriate functional forms can be determined for the reduced parameters, it is far better to simultaneously use data for many fluids to determine the resultant generalized parameters in these functional forms. This approach was used in the present research.

Correlation of Reduced Parameters as Generalized Functions of Acentric Factor

The relatively well behaved functionality between the reduced parameters and acentric factors for several of the parameters in Figure II-1 suggests the linear relations in Equations (II-4)-(II-14) can be used to correlate the reduced parameters in terms of the component acentric factor, ω_i, critical temperatures, T_{c_i}, and critical density, ρ_{c_i}. The need for the

nonlinear relation in Equation (II-14) will be discussed subsequently.

$$\rho_{ci} B_{oi} = A_1 + B_1 \omega_i \tag{II-4}$$

$$\frac{\rho_{ci} A_{oi}}{RT_{ci}} = A_2 + B_2 \omega_i \tag{II-5}$$

$$\frac{\rho_{ci} C_{oi}}{RT^3_{ci}} = A_3 + B_3 \omega_i \tag{II-6}$$

$$\rho^2_{ci} \gamma_i = A_4 + B_4 \omega_i \tag{II-7}$$

$$\rho^2_{ci} b_i = A_5 + B_5 \omega_i \tag{II-8}$$

$$\frac{\rho^2_{ci} a_i}{RT_{ci}} = A_6 + B_6 \omega_i \tag{II-9}$$

$$\rho^3_{ci} \alpha_i = A_7 + B_7 \omega_i \tag{II-10}$$

$$\frac{\rho^2_{ci} c_i}{RT^3_{ci}} = A_8 + B_8 \omega_i \tag{II-11}$$

$$\frac{\rho_{ci} D_{oi}}{RT^4_{ci}} = A_9 + B_9 \omega_i \tag{II-12}$$

$$\frac{\rho^2_{ci} d_i}{RT^2_{ci}} = A_{10} + B_{10} \omega_i \tag{II-13}$$

$$\frac{\rho_{ci} E_{oi}}{RT^5_{ci}} = A_{11} + B_{11} \omega_i \exp(-3.8\omega_i) \tag{II-14}$$

The high interdependence among the reduced parameters for a given fluid suggests the feasibility of determining an aggregate set of generalized parameters (A_j and B_j, j = 1,2, ... 11) using data for several fluids, such that the reduced parameters conform to the assumed functionality with acentric factor. In addition, by using multiproperty analysis for their determination, the set of generalized parameters may be used to predict all thermodynamic properties rather than PVT behavior only, as has been the case traditionally[96]. To this end, multiproperty regression analysis was used to determine the generalized parameters in Equations (II-4)-(II-14). To minimize computer core storage and execution time, only the normal paraffins methane through n-octane were used to generate the coefficients in the parameter expressions in Equations (II-4)-(II-14). Nevertheless, almost 400 carefully selected PVT, enthalpy and vapor pressure data points were used in the computation.

The following function was minimized in the multiproperty regression calculations[57].

$$Q = \sum_{i}^{NC} \sum_{j}^{(NP)_i} \left[1 - \frac{\rho_{calc,ij}}{\rho_{exp,ij}}\right]^2 + \sum_{i}^{NC} \sum_{j}^{(NP)_i} \left[1 - \frac{(H-H^o)_{calc,ij}}{(H-H^o)_{exp,ij}}\right]^2 + \sum_{i}^{NC} \sum_{j}^{(NP)_i} \left[1 - \frac{f_{ij}^L}{f_{ij}^V}\right]^2 \qquad \text{(II-15)}$$

In Equation (II-15), NC is the number of pure components used in the regression and $(NP)_i$ is the number of data points of the i^{th} component for each property. Descriptions of computational procedures and computer programs for multiproperty analysis have been discussed in a number of literature sources.[10,18,21,56,57,65,96,97,99]

The parameters A_j and B_j (j = 1,2, ..., 11) in Equations (II-4)-(II-14) determined in the regression calculations are given in Table II-1. The value of $A_{11} + B_{11}\,\omega_i$ is negative for values of the acentric factor ω_i larger than 0.29. Since the use of negative parameter values for individual fluids is inconvenient in calculations of mixture parameters, multiplication of B_{11} by the correction factor "exp(-3.8 ω_i)" was necessary. The correction term for B_{11} was determined by searching for optimum E_o' values for each of the eight pure fluids, using a trial-and-error method, followed by correlation of the optimum E_o' values found, using Equation (II-14). The values of critical temperature, T_{ci}, critical density, ρ_{ci}, and acentric factor, ω_i, used in these calculations are given in Table II-2. For consistency in thermodynamic property prediction calculations, the values of T_{ci}, ρ_{ci} and ω_i given in Table II-2 should be used with the correlation. In particular, the values of ω_i in Table II-2 should be used, since there is considerable disagreement in acentric factor values reported in standard references. Because of the noted disagreement in reported acentric factors, values of the characterization parameter ω_i consistent with the present correlation have been determined and are given in Table II-2 for twenty-six fluids. The determination of the characterization parameter ω_i also can be carried out using a trial-and-error method. Comparison of calculated saturated fugacity values of liquid (f^L) and vapor (f^V) can make this step a lot easier.

If $f^L > f^V$ along the vapor pressure curve, the pressures chosen (i.e. experimental vapor pressures) are lower than the vapor pressures predicted by the equation of state, therefore the ω_i value used should be increased in order to reduce f^L, and conversely if $f^L < f^V$, the ω_i value should be

TABLE II-1

VALUES OF GENERALIZED PARAMETERS A_j AND B_j FOR USE WITH GENERALIZED EQUATION OF STATE

Parameter Subscript(j)	Parameter Value	
	A_j	B_j
1	0.443690	0.115449
2	1.28438	-0.920731
3	0.356306	1.70871
4	0.544979	-0.270896
5	0.528629	0.349261
6	0.484011	0.754130
7	0.0705233	-0.044448
8	0.504087	1.32245
9	0.0307452	0.179433
10	0.0732828	0.463492
11	0.006450	-0.022143

TABLE II-2

PHYSICAL PROPERTIES OF PURE MATERIALS USED WITH GENERALIZED EQUATION OF STATE

	Critical Temp., °F	Critical Density lb-mole/ cu.ft.	Molecular Weight	Acentric Factor
Methane	-116.43	0.6274	16.042	0.013
Ethane	90.03	0.4218	30.068	0.1018
Propane	206.13	0.3121	44.094	0.157
i-Butane	274.96	0.2373	58.12	0.183
n-Butane	305.67	0.2448	58.12	0.197
i-Pentane	369.	0.2027	72.146	0.226
n-Pentane	385.42	0.2007	72.146	0.252
n-Hexane	453.45	0.1696	86.172	0.302
n-Heptane	512.85	0.1465	100.198	0.353
n-Octane	563.79	0.1284	114.224	0.412
n-Nonane	610.5	0.1150	128.25	0.475
N-Decane	651.9	0.1037	142.276	0.54
n-Undecane	692.31	0.0946	156.30	0.6
Ethylene	49.82	0.5035	28.05	0.101
Propylene	197.4	0.3449	42.08	0.15
Nitrogen	-232.6	0.6929	28.016	0.035
Carbon Dioxide	87.8	0.6641	44.01	0.21
Hydrogen Sulfide	212.7	0.6571	34.076	0.105
Cyclohexane	535.6	0.2027	84.156	0.210
Benzene	552.	0.2401	78.108	0.215
Nitrous Oxide	97.77	0.6483	44.02	0.155
Nitric Oxide	-135.69	1.0764	30.01	0.600
Toluene	605.5	0.1924	92.134	0.260
Sulfur Dioxide	315.5	0.5118	64.06	0.273
Methyl Chloride	289.65	0.4366	50.49	0.17
Ethylene Oxide	382.71	0.4524	44.05	0.157

reduced. Generally, the resultant optimum value of ω is near the values of acentric factors reported in the literature.

Sensitivities of Saturated Properties to Reduced Parameters

The parameter sensitivity study presented here has played a significant role in the determination of the optimal parameter values through regression analysis. Because the sensitivities of thermodynamic properties to each reduced parameter are different, the study helps to provide a guide or basis for selection of parameters which should be modified for improved predictions in a given temperature (or density) region.

The measure of sensitivity used was the percent change in the thermodynamic properties at saturated conditions for a one percent change in the reduced parameter being considered. The property which is most sensitive to parameter variation is the liquid fugacity. This sensitivity is shown in Figure II-2 for propane. Figure II-2 demonstrates clearly that modification of the reduced parameter E_o' can significantly affect liquid fugacity calculations below $T_r = 0.4$, while making only small changes at higher reduced temperatures.

Application of the Generalized Correlation to Mixtures

Correlation of mixture behavior using the generalized equation of state requires characterization of the mixture on the basis of the characteristics and amounts of the components in the mixture. The method most commonly used in the past has been to treat the mixture parameters as functions

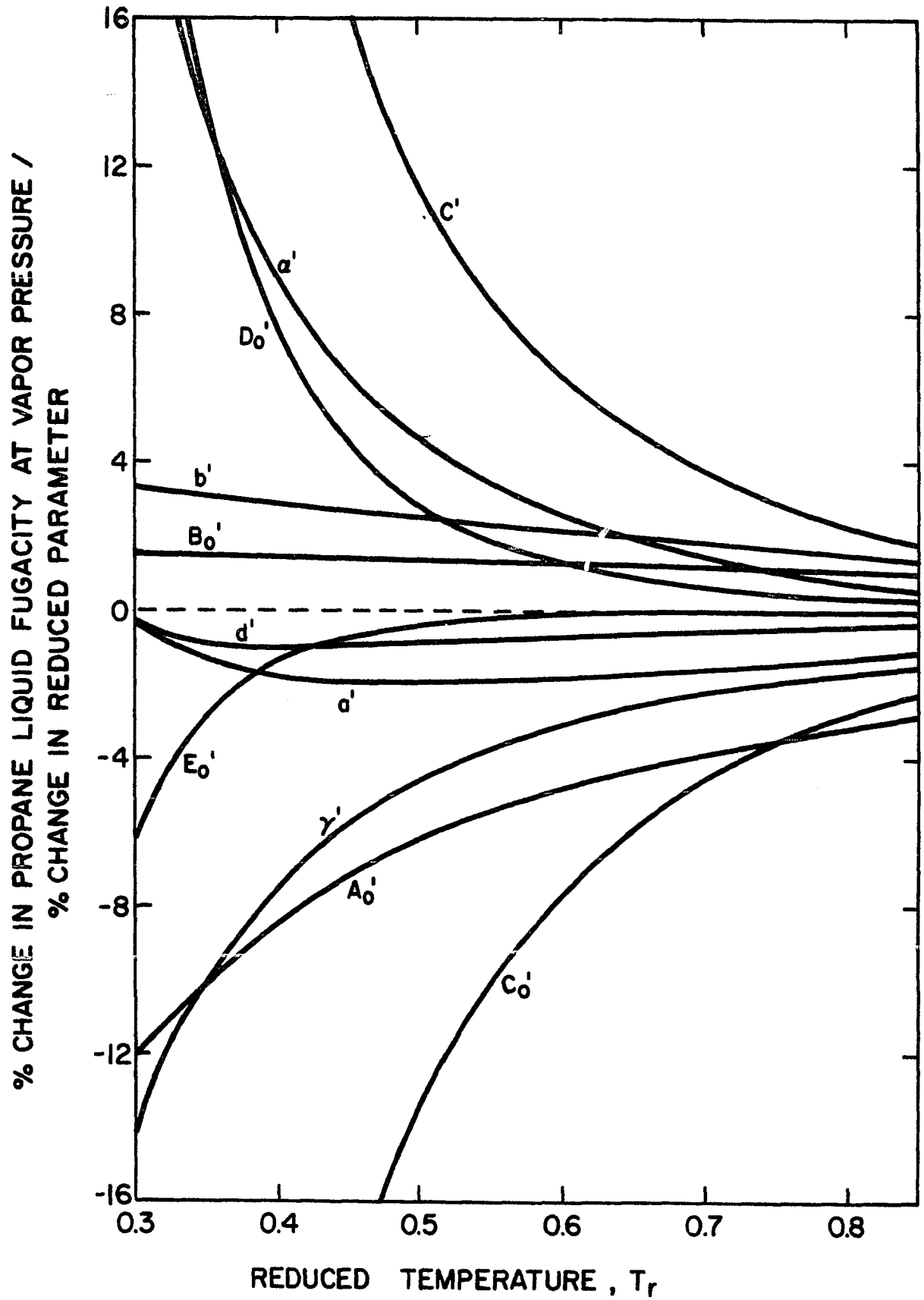

Figure II-2 Sensitivity of Liquid Fugacity at Vapor Pressure to the Reduced Equation of State Parameters.

of composition, the pure component parameters, and unlike interaction parameters. This is the method used by Benedict, Webb, and Rubin[5] in their work with the BWR equation.

Quite recently, Bishnoi and Robinson[8] have developed very successful new mixing rules for the BWR equation. These new mixture parameter equations have been quite useful for the prediction of high temperature K-values for systems containing hydrogen sulfide, carbon dioxide, and nitrogen. Since the generalized equation presented here has the same density dependence as the BWR equation it was anticipated that the type of mixing rule proposed by Robinson could be used successfully in Equation (II-1). Calculations for a large number of systems have shown that this new formulation for mixing rules is a viable approach for predicting mixture behavior. However, use of the mixing rules proposed by Bishnoi and Robinson requires excessive amounts of computing time in vapor-liquid equilibrium calculations for systems of more than three components. This is due to the need for repetitious calculations of triple summations involved in the expressions for a, c and d.

The following relations can be written for the eleven mixture parameters in the new equation of state, using nomenclature analogous to that of Bishnoi and Robinson[8].

$$B_o = \sum_{i=1}^{n} \sum_{j=1}^{n} x_i x_j B_{oij} \qquad \text{(II-16)}$$

$$A_o = \sum_{i=j}^{n} \sum_{j=1}^{n} x_i x_j A_{oij} \qquad \text{(II-17)}$$

$$C_o = \sum_{i=1}^{n} \sum_{j=1}^{n} x_i x_j C_{oij} \qquad \text{(II-18)}$$

$$\gamma = \sum_{i=1}^{n} \sum_{j=1}^{n} x_i x_j \gamma_{ij} \qquad \text{(II-19)}$$

$$b = \sum_{i=1}^{n} \sum_{j=1}^{n} \sum_{k=1}^{n} x_i x_j x_k (b_{ij} b_{jk} b_{ik})^{1/3} \qquad \text{(II-20)}$$

$$a = \sum_{i=1}^{n} \sum_{j=1}^{n} \sum_{k=1}^{n} x_i x_j x_k (a_{ij} a_{jk} a_{ik})^{1/3} \qquad \text{(II-21)}$$

$$\alpha = \sum_{i=1}^{n} \sum_{j=1}^{n} \sum_{j=1}^{n} x_i x_j x_k (\alpha_{ij} \alpha_{jk} \alpha_{ik})^{1/3} \qquad \text{(II-22)}$$

$$c = \sum_{i=1}^{n} \sum_{j=1}^{n} \sum_{k=1}^{n} x_i x_j x_k (c_{ij} c_{jk} c_{ik})^{1/3} \qquad \text{(II-23)}$$

$$D_o = \sum_{i=1}^{n} \sum_{j=1}^{n} x_i x_j D_{oij} \qquad \text{(II-24)}$$

$$d = \sum_{i=1}^{n} \sum_{j=1}^{n} \sum_{k=1}^{n} x_i x_j x_k (d_{ij} d_{jk} d_{ik})^{1/3} \qquad \text{(II-25)}$$

$$E_o = \sum_{i=1}^{n} \sum_{j=1}^{n} x_i x_j E_{oij} \qquad \text{(II-26)}$$

In Equations (II-16)-(II-26), x_i is the mole fraction of the i^{th} component and n is the total number of components. In the present work, the binary interaction parameters B_{oij}, A_{oij}, etc. have been treated as the following functions of the pure component parameters B_{oi}, A_{oi}, etc. and the interaction parameter k_{ij}, which will be discussed subsequently.

$$B_{oij} = \tfrac{1}{2}(B_{oi}+B_{oj}) \qquad \text{(II-27)}$$

$$A_{oij} = \sqrt{A_{oi}A_{oj}}\,(1-k_{ij}) \qquad \text{(II-28)}$$

$$C_{oij} = \sqrt{C_{oi}C_{oj}}\,(1-k_{ij})^3 \qquad \text{(II-29)}$$

$$\gamma_{ij} = \sqrt{\gamma_i \gamma_j} \tag{II-30}$$

$$b_{ij} = \sqrt{b_i b_j} \tag{II-31}$$

$$a_{ij} = \sqrt{a_i a_j} \tag{II-32}$$

$$\alpha_{ij} = \sqrt{\alpha_i \alpha_j} \tag{II-33}$$

$$c_{ij} = \sqrt{c_i c_j} \tag{II-34}$$

$$D_{oij} = \sqrt{D_{oi} D_{oj}}\,(1 - k_{ij})^4 \tag{II-35}$$

$$d_{ij} = \sqrt{d_i d_j} \tag{II-36}$$

$$E_{oij} = \sqrt{E_{oi} E_{oj}}\,(1 - k_{ij})^5 \tag{II-37}$$

Equations (II-16) through (II-37) can be reduced to Equations (II-38)-(II-48) for practical computation.

$$B_o = \sum_{i=1}^{n} x_i B_{oi} \tag{II-38}$$

$$A_o = \sum_{i=1}^{n} \sum_{j=1}^{n} x_i x_j A_{oi}^{1/2} A_{oj}^{1/2} (1 - k_{ij}) \tag{II-39}$$

$$C_o = \sum_{i=1}^{n} \sum_{j=1}^{n} x_i x_j C_{oi}^{1/2} C_{oj}^{1/2} (1 - k_{ij})^3 \tag{II-40}$$

$$\gamma = \left[\sum_{i=1}^{n} x_i \gamma_i^{1/2} \right]^2 \tag{II-41}$$

$$b = \left[\sum_{i=1}^{n} x_i b_i^{1/3} \right]^3 \tag{II-42}$$

$$a = \left[\sum_{i=1}^{n} x_i a_i^{1/3}\right]^3 \tag{II-43}$$

$$\alpha = \left[\sum_{i=1}^{n} x_i \alpha_i^{1/3}\right]^3 \tag{II-44}$$

$$c = \left[\sum_{i=1}^{n} x_i c_i^{1/3}\right]^3 \tag{II-45}$$

$$D_o = \sum_{i=1}^{n} \sum_{j=1}^{n} x_i x_j D_{oi}^{1/2} D_{oj}^{1/2} (1 - k_{ij})^4 \tag{II-46}$$

$$d = \left[\sum_{i=1}^{n} x_i d_i^{1/3}\right]^3 \tag{II-47}$$

$$E_o = \sum_{i=1}^{n} \sum_{j=1}^{n} x_i x_j E_{oi}^{1/2} E_{oj}^{1/2} (1 - k_{ij})^5 \tag{II-48}$$

Use of exact analogs of the expressions presented by Bisnoi and Robinson would require the following expressions for B_{oij}, a_{ij}, c_{ij} and d_{ij}.

$$B_{oij} = \sqrt{B_{oi} B_{oj}} \tag{II-49}$$

$$a_{ij} = \sqrt{a_i a_j}\ (1 - k_{ij}) \tag{II-50}$$

$$c_{ij} = \sqrt{c_i c_j}\ (1 - k_{ij})^3 \tag{II-51}$$

$$d_{ij} = \sqrt{d_i d_j}\ (1 - k_{ij})^2 \tag{II-52}$$

Use of these Equations (II-49)-(II-52) leads to the following expressions for B_o, a, c and d.

$$B_o = \sum_{i=1}^{n} \sum_{j=1}^{n} x_i x_j \sqrt{B_{oi} B_{oj}} \tag{II-53}$$

$$a = \sum_{i=1}^{n} \sum_{j=1}^{n} \sum_{k=1}^{n} x_i x_j x_k \, a_i^{1/3} \, a_j^{1/3} \, a_k^{1/3} \, (1 - k_{ij})^{1/3} \, (1 - k_{jk})^{1/3} \, (1 - k_{ik})^{1/3} \qquad \text{(II-54)}$$

$$c = \sum_{i=1}^{n} \sum_{j=1}^{n} \sum_{k=1}^{n} x_i x_j x_k \, c_i^{1/3} \, c_j^{1/3} \, c_k^{1/3} \, (1 - k_{ij}) \, (1 - k_{jk}) \, (1 - k_{ik}) \qquad \text{(II-55)}$$

$$d = \sum_{i=1}^{n} \sum_{j=1}^{n} \sum_{k=1}^{n} x_i x_j x_k \, d_i^{1/3} \, d_j^{1/3} \, d_k^{1/3} \, (1 - k_{ij})^{2/3} \, (1 - k_{jk})^{2/3} \, (1 - k_{ik})^{2/3} \qquad \text{(II-56)}$$

It is the use of triple summations in Equations (II-54)-(II-56) that leads to excessive computer time in multicomponent vapor-liquid equilibrium calculations. For example, for a fifteen component system (such as normally encountered in absorber calculations), there are $(15)^3 = 3375$ terms involved in the expression for c used by Bishnoi and Robinson, Equation (II-55), while there are only 15 terms in the expression for c used in present work, Equation (II-45). Thus, for economic reasons alone, the use of triple summations in expression for mixture parameters must be prohibited in computer programs. Fortunately, mixing rules (Equations (II-38)-(II-48)) used in the present work not only shorten computing time significantly compared to the Bishnoi and Robinson rules but also (for the equation of state used here) predict thermodynamic properties more accurately than the rules involving triple summations.

The interaction parameter k_{ij} is a measure of deviations from ideal solution behavior for interactions between the i^{th} and j^{th} components[8,80]. Thus, k_{ij} is zero when i equals j (pure fluid interaction) and k_{ij} is near zero for component pairs which form nearly ideal solutions (for example,

paraffin hydrocarbon pairs heavier than propane). The numerical value of k_{ij} differs considerable from zero when the component pair forms highly nonideal solutions. Thus, accurate values of k_{ij} are required when i or j is a light hydrocarbon or a nonhydrocarbon. Compared to vapor-liquid equilibrium predictions, the sensitivity of predicted bulk mixture properties such as density and enthalpy to the value of k_{ij} is small. Therefore, binary vapor-liquid equilibrium data have been relied on principally for determining k_{ij} values. Tabulations of k_{ij} values for component pairs encountered in the hydrocarbon processing industry are presented in Table II-3.

Figure VI-3 illustrates the effect of variation in the interaction parameter k_{ij} on K-values for the methane-hydrogen sulfide system. The improvement in methane K-values using $k_{ij} = 0.05$ over the use of $k_{ij} = 0.00$ is significant. On the other hand, hydrogen sulfide K-values are virtually unaffected by this variation in k_{ij}. It has been noted in general that K-values of components occurring in larger percentages in the vapor phase are affected by variations in k_{ij} to a greater extent than components occurring in smaller percentages in the vapor phase.

TABLE II-3

VALUES OF INTERACTION PARAMETERS k_{ij} FOR USE IN GENERALIZED CORRELATION ($k_{ij} \times 100$)

Methane	Ethylene	Ethane	Propylene	Propane	i-Butane	n-Butane	i-Pentane	n-Pentane	Hexane	Heptane	Octane	Nonane	Decane	Undecane	Nitrogen	Carbon Dioxide	Hydrogen Sulfide	
0.0	1.0	1.0	2.1	2.3	2.75	3.1	3.6	4.1	5.0	6.0	7.0	8.1	9.2	10.1	2.5	5.0	5.0	Methane
	0.0	0.0	0.3	0.31	0.4	0.45	0.5	0.6	0.7	0.85	1.0	1.2	1.3	1.5	7.0	4.8	4.5	Ethylene
		0.0	0.3	0.31	0.4	0.45	0.5	0.6	0.7	0.85	1.0	1.2	1.3	1.5	7.0	4.8	4.5	Ethane
			0.0	0.0	0.3	0.35	0.4	0.45	0.5	0.65	0.8	1.0	1.1	1.3	10.0	4.5	4.0	Propylene
				0.0	0.3	0.35	0.4	0.45	0.5	0.65	0.8	1.0	1.1	1.3	10.0	4.5	4.0	Propane
					0.0	0.0	0.08	0.1	0.15	0.18	0.2	0.25	0.3	0.3	11.0	5.0	3.6	i-Butane
						0.0	0.08	0.1	0.15	0.18	0.2	0.25	0.3	0.3	12.0	5.0	3.4	n-Butane
							0.0	0.0	0.0	0.0	0.0	0.0	0.0	0.0	13.4	5.0	2.8	i-Pentane
								0.0	0.0	0.0	0.0	0.0	0.0	0.0	14.8	5.0	2.0	n-Pentane
									0.0	0.0	0.0	0.0	0.0	0.0	17.2	5.0	0.0	Hexane
										0.0	0.0	0.0	0.0	0.0	20.0	5.0	0.0	Heptane
											0.0	0.0	0.0	0.0	22.8	5.0	0.0	Octane
												0.0	0.0	0.0	26.4	5.0	0.0	Nonane
													0.0	0.0	29.4	5.0	0.0	Decane
														0.0	32.2	5.0	0.0	Undecane
															0.0	0.0	0.0	Nitrogen
																0.0	3.5	Carbon Dioxide
																	0.0	Hydrogen Sulfide

CHAPTER III

AN EFFICIENT DENSITY SEARCH METHOD

For practical applications using the generalized correlation, it is very important that computing time for repetitious calculations be minimized. For this reason, efficient computer programming is mandatory for all calculations which utilize search techniques. Density calculation is the most frequently called search calculation, because in estimating other thermodynamic properties (enthalpy, entropy and fugacity) density must be determined for a given temperature and pressure before the other properties can be calculated. Various density search methods are briefly discussed here and a new density search method is presented.

Since the equation of state (Equation II-1) is implicit in density, an iterative scheme is required for density calculation. Three iterative methods, the false-position method, Newton-Raphson method and trial-and-error method, were considered for use in density calculations. To test the speed of convergence, comparison calculations of the three methods were made.

Equation II-1 can possess three or more density roots at all temperatures below the critical temperature. Only the smallest and largest roots have physical significance, corresponding to vapor and liquid densities, respectively.

In the trial-and-error method of density calculation[43], for the vapor phase, an initial density estimate of zero was used, with equal increments (e.g., the smaller of 0.1 P/RT and 0.01 lb-moles/cu.ft.) added to the density in the iterative procedure until the calculated pressure exceeded the actual pressure. The density was then reduced by the final increment, the increment was reduced through division by ten and then the new increment was added to the density iteratively until the calculated pressure again exceeded the actual pressure. This procedure was continued until the density increment size reached a specified small value (e.g., 0.000001 lb.-mole/cu.ft.). For the liquid phase, the procedure for solving for the density is similar except that the initial density estimate was chosen to be larger than ever actually encountered and increments are subtracted rather than added in the iterative procedure. The initial liquid density estimate of 2.0 lb.-moles/cu.ft. and initial increment size of 0.05 lb.-mole/cu.ft. were used.

In the Newton-Raphson method[58], the first derivative of pressure with respect to density was calculated analytically at each iteration step. The density increment was the ratio of the difference in the desired pressure and the calculated pressure, divided by the derivative of pressure with respect to density. The initial density estimates used in the Newton-Raphson method were identical to those used in the trial-and-error method.

The false-position method[58] is similar to the Newton-Raphson method. However, each iteration is faster because the derivative is merely estimated as the ratio of the pressure increment to the density increment from the previous iteration, rather than being calculated analytically.

In comparison tests of the three iterative density search methods using the generalized equation, the false-position method was found to be slightly faster than the Newton-Raphson method in most regions of density. Both the false position and Newton-Raphson methods were orders of magnitude faster than the trial-and-error method. However, the trial-and-error method is more commonly used for industrial calculations because most programs written using the two faster methods fail in certain cases. Therefore, use of the false-position method in the generalized correlation required for fail-safe, self-protective density search subroutine. A careful study of isothermal pressure-density behavior led to the construction of a simple scheme and program for this purpose. Although the scheme lacks a rigorous convergence proof, the actual use of the program without failure proved the scheme to be truly workable.

A self-explanatory flow sheet for the fail-safe false-position density search program is presented in Figure III-1. Pressure (P), temperature (T), acentric factor (ω) and the density key (MD=0 if vapor, and MD=-1 if liquid) are needed in the density search program. FN(i) is defined to be the calculated pressure using Equation II-1 for the density value at the i^{th} iteration minus the given pressure. In Figure III-1, the blocks enclosed by dotted lines were added as safety precautions against internal loopings, etc., although the use of those blocks never occurred. If internal looping (KK=2) should occur, the trial-and-error density search method (DENTE) is called.

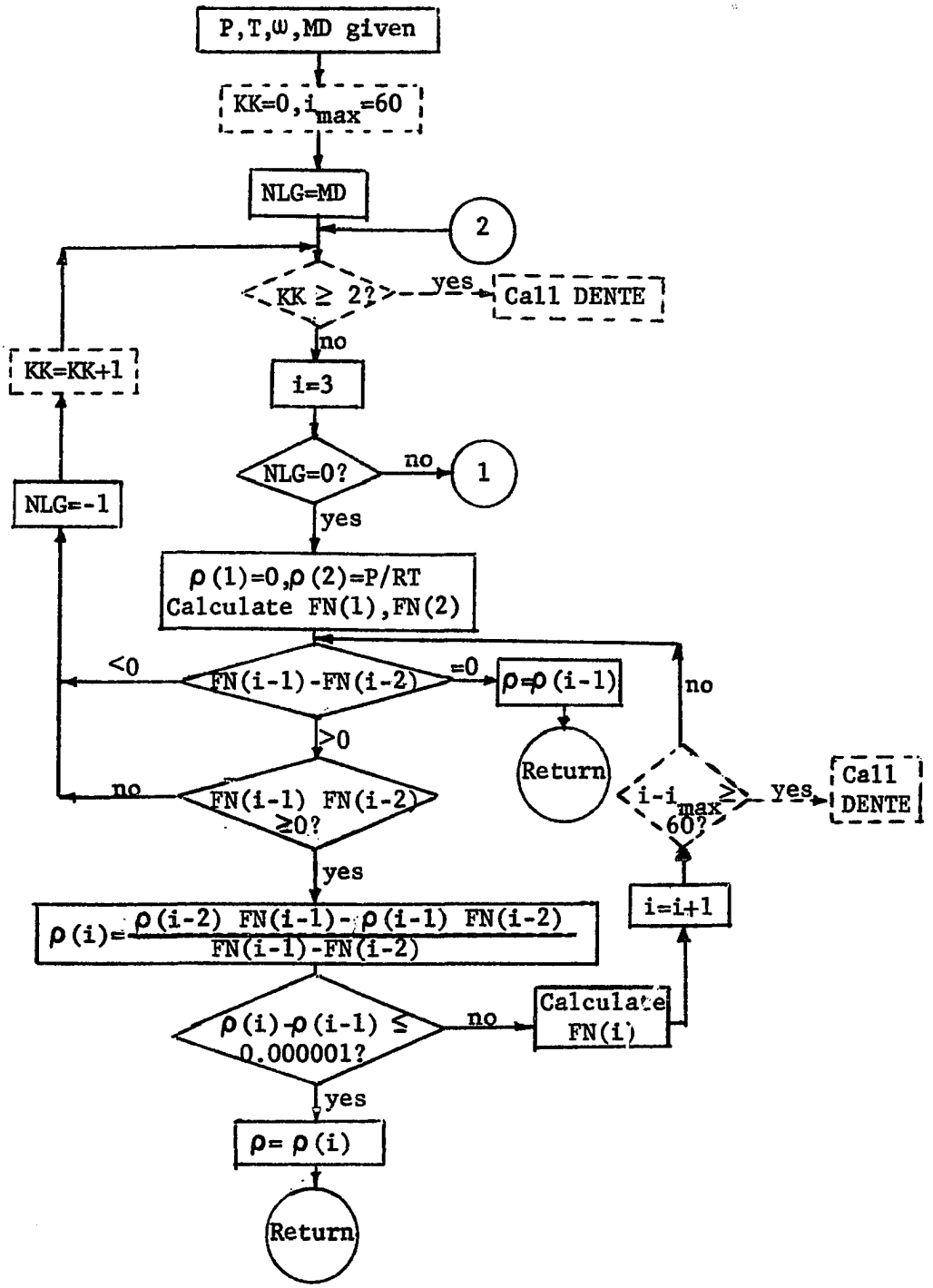

Figure III-1. Flow Sheet for Density Search Program Using False-Position Method

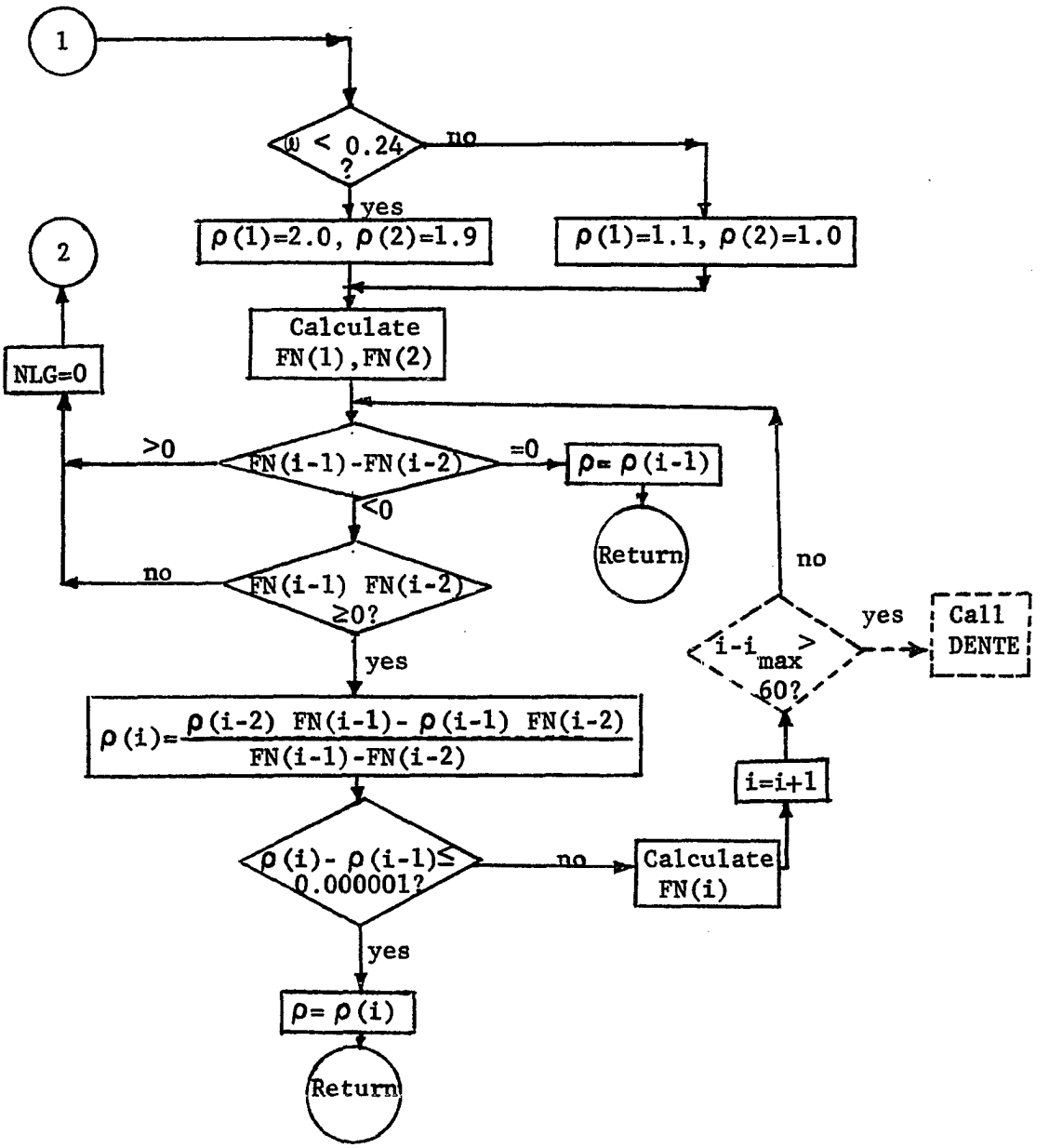

Figure III-1. (Continued)

CHAPTER IV

USE OF CRITICAL CONSTRAINTS IN DETERMINATIONS OF GENERALIZED PARAMETERS

Accurate prediction of thermodynamic behavior near the critical region is often necessary in engineering design calculations. The generalized correlation predicts the critical temperatures of the light paraffins methane through n-butane within a few degrees. However, the predicted critical temperatures of fluids heavier than pentane are in error by more than $10^{o}F$ in some cases. The purpose of the material presented here is to show that an exact fit of critical conditions can be obtained by the use of critical constraints.

At the critical point, the following three conditions must be satisfied.

$$P_c = (P(T,\rho, \{A\}))_{T=T_c,\rho=\rho_c} \tag{IV-1}$$

$$\left(\frac{\partial P}{\partial \rho}\right)_{T_c,\rho_c} = 0 \tag{IV-2}$$

$$\left(\frac{\partial^2 P}{\partial \rho^2}\right)_{T_c,\rho_c} = 0 \tag{IV-3}$$

Application of these three conditions to the generalized correlation yields the following relations.

$$\frac{P_c}{\rho_c RT_c} = 1 + (B_o' - A_o' - C_o' - D_o' - E_o') + (b' - a' - d') + \alpha'(a' + d') + c'(1 + \gamma') \exp(-\gamma') \quad \text{(IV-4)}$$

$$0 = 1 + 2(B_o' - A_o' - C_o' + D_o' - E_o') + 3(b' - a' - d') + 6\alpha'(a' + d') + c'(3 + 3\gamma' - 2\gamma'^2) \exp(-\gamma') \quad \text{(IV-5)}$$

$$0 = 2(B_o' - A_o' - C_o' + D_o' - E_o') + 6(b' - a' - d') + 30\alpha'(a' + d') + 2c'(3 + 3\gamma' - 9\gamma'^2 + 2\gamma'^3) \exp(-\gamma') \quad \text{(IV-6)}$$

Rearranging the Equations (IV-4)-(IV-6) for B_o', b' and c' results in the following three non-trivial simultaneous equations.

$$B_o' + b' + c'(1+\gamma')\exp(-\gamma') = \frac{P_c}{\rho_c RT_c} - 1 + (A_o' + C_o' - D_o' + E_o') + a' + d' - \alpha'(a' + d') \quad \text{(IV-7)}$$

$$2B_o' + 3b' + c'(3 + 3\gamma' - 2\gamma'^2)\exp(-\gamma') = -1 + 2(A_o' + C_o' - D_o' + E_o') + 3(a' + d') - 6\alpha'(a' + d') \quad \text{(IV-8)}$$

$$2B_o' + 6b' + c'(6 + 6\gamma' - 18\gamma'^2 + 4\gamma'^3)\exp(-\gamma') = 2(A_o' + C_o' - D_o' + E_o') + 6(a' + d') - 30\alpha'(a' + d') \quad \text{(IV-9)}$$

The three reduced parameters B_o', b' and c' are expressed in terms of the remaining eight reduced parameters in these critical constraint relations Equations (IV-7)-(IV-9). The values of B_o', b' and c' for methane and normal pentane determined from solving the three critical constraint equations are compared with the previous nonconstrained values determined in Table IV-1.

Inspection of Table IV-1 indicates that the disagreement between two sets of values is not great. Thermodynamic property calculations using B_o', b' and c' determined with critical constraints yield excellent predictions between the reduced temperature 0.83 and the critical temperature. For lower temperatures, predictions rapidly become very poor. This is due principally to the fact that thermodynamic properties are very sensitive to the parameter c' at lower temperatures.

If one desires an exact fit of critical conditions as well as accurate thermodynamic property predictions down to reduced temperature as low as 0.3 using the generalized correlation, values of B_o', b' and c' determined from the critical constraints can be used above the reduced temperature 0.83.

TABLE IV-1

COMPARISONS OF VALUES OF THE REDUCED PARAMETERS B'_o, b' AND c' DETERMINED WITH AND WITHOUT CRITICAL CONSTRAINTS

		Without Critical Constraints	With Critical Constraints
Methane	B'_o	0.445191	0.430481
	b'	0.533168	0.525201
	c'	0.521279	0.549144
n-Pentane	B'_o	0.472783	0.480424
	b'	0.616643	0.564495
	c'	0.837344	0.877458

CHAPTER V

COMPUTATIONAL PROCEDURES FOR PREDICTING FLUID THERMODYNAMIC BEHAVIOR USING THE GENERALIZED CORRELATION

Methods for predicting fluid thermodynamic properties and vapor-liquid equilibria using the generalized correlation are presented here along with the necessary equations.

The basic equations for use of the generalized correlation in prediction of thermodynamic properties are Equation II-1 and Equations (II-4)-(II-14). Equations for calculation of all thermodynamic properties can be derived from these basic equations with the use of fundamental thermodynamic relationships.

Density

Calculation procedures for density are presented in Chapter III.

Enthalpy

The enthalpy of a compound is calculated using the equation

$$H = (H - H^o) + (H^o - H^o_o) + H^o_o \qquad \text{(V-1)}$$

H^o_o is the standard enthalpy of formation of the compound from the elements at 0 psia and 0^oR, and is obtained from API[90]. $(H^o - H^o_o)$ is the difference in the enthalpy of the compound in the ideal gas state at the temperature of interest and the reference state of 0^oR. The ideal gas enthalpy difference

$(H^o - H^o_o)$ also is obtained from API[90]. $(H - H^o)$, the enthalpy departure, is the difference in the enthalpy of the compound at the temperature-pressure condition of interest and the enthalpy of the compound in the ideal gas state at the same temperature.

The enthalpy departure is related to the equation of state by the following equation[38].

$$(H - H^o) = P/\rho - RT + \int_o^\rho \left[P - T\left(\frac{\partial P}{\partial T}\right)_\rho\right] \frac{d\rho}{\rho^2} \qquad \text{(V-2)}$$

When the new equation of state given in Equation II-1 is used in Equation V-2, the equation of state expression for the enthalpy departure has the form

$$(H - H^o) = \left(B_o RT - 2A_o - \frac{4C_o}{T^2} + \frac{5D_o}{T^3} - \frac{6E_o}{T^4}\right)\rho$$

$$+ \frac{1}{2}\left(2bRT - 3a - \frac{4d}{T}\right)\rho^2 + \frac{1}{5}\alpha\left(6a + \frac{7d}{T}\right)\rho^5 \qquad \text{(V-3)}$$

$$+ \frac{c}{\gamma T^2}\left[3 - \left(3 + \frac{1}{2}\gamma\rho^2 - \gamma^2\rho^4\right)\exp(-\gamma\rho^2)\right]$$

For self-consistency, the density value used in Equation V-3 for calculation of the enthalpy departure must be determined by the solution of Equation II-1 for the temperature-pressure condition of interest. The computer programming necessary for the calculation of enthalpy is straightforward. The procedure has been discussed in detail for the BWR equation by Johnson and Colver[43].

Entropy

The entropy of a compound is calculated using the equation

$$S = (S - S^o) + S^o \qquad \text{(V-4)}$$

This equation is entirely analogous to Equation V-1 for the enthalpy except that the entropy of formation at $0^{o}R$, S_{o}^{o}, is zero by virtue of the third law of thermodynamics[14]. S^{o} is the entropy of the compound in the ideal gas state at unit pressure[14] and is obtained from API[90]. The entropy departure $(S - S^{o})$ is the difference in the entropy of the compound at the temperature-pressure condition of interest and the entropy of the compound in the ideal gas state at the same temperature and unit pressure. The entropy departure is related to the equation of state by the following equation[38]

$$(S - S^{o}) = -R \ln (\rho RT) + \int_{0}^{\rho} \left[\rho R - \left(\frac{\partial P}{\partial T}\right)_{\rho}\right] \frac{d\rho}{\rho^{2}} \qquad \text{(V-5)}$$

When the new equation of state given in Equation II-1 is used in Equation V-5, the equation of state expression for the entropy departure has the form

$$(S - S^{o}) = -R \ln (\rho RT) - \left(B_{o}R + \frac{2C_{o}}{T^{3}} - \frac{3D_{o}}{T^{4}} + \frac{4E_{o}}{T^{5}}\right) \rho$$

$$- \frac{1}{2} \left(bR + \frac{d}{T^{2}}\right) \rho^{2} + \frac{\alpha d \rho^{5}}{5T^{2}} \qquad \text{(V-6)}$$

$$+ \frac{2c}{\gamma T^{3}} \left[1 - \left(1 + \frac{1}{2} \gamma \rho^{2}\right) \exp\left(-\gamma \rho^{2}\right)\right]$$

The density value used in Equation V-6 should be determined by solution of Equation II-1. Computer calculations of entropy departures can be made easily, following the procedure utilized by Johnson and Colver for enthalpy departures[43].

Fugacity

The fugacity may be expressed in terms of the enthalpy departure and entropy departure by the thermodynamic relation

$$RT \ln f = (H - H^{o}) - T(S - S^{o}) \qquad \text{(V-7)}$$

Thus, using Equations V-2 and V-6 in Equation V-7, the equation of state expression for the fugacity has the form

$$RT \ln f = RT \ln (\rho RT) + 2\left(B_o RT - A_o - \frac{C_o}{T^2} + \frac{D_o}{T^3} - \frac{E_o}{T^4}\right)\rho$$

$$+ \frac{3}{2}\left(bRT - a - \frac{d}{T}\right)\rho^2 + \frac{6\alpha}{5}\left(a + \frac{d}{T}\right)\rho^5 \qquad \text{(V-8)}$$

$$+ \frac{C}{\gamma T^2}\left[1 - \left(1 - \frac{1}{2}\gamma\rho^2 - \gamma^2\rho^4\right)\exp\left(-\gamma\rho^2\right)\right]$$

As was also noted for enthalpy and entropy, the density value used in Equation V-8 for computing the fugacity should be determined by solving Equation II-1.

Vapor Pressure

Determination of the vapor pressure P_s at a given temperature requires the simultaneous solution of the following condition equations for vapor-liquid equilibrium[4],

$$P^L = P^V = P_s \qquad \text{(V-9)}$$

$$f^L = f^V \qquad \text{(V-10)}$$

where L and V refer to liquid and vapor, respectively. The following trial-and-error procedure can be carried out easily by computer. To start the procedure, an initial estimate of the vapor pressure P_s is made. Then P^L and P^V are set equal to P_s to satisfy Equation V-9. Liquid and vapor densities (ρ^L and ρ^V) are then calculated by solving for the largest and smallest roots satisfying Equation II-1, with $P = P_s$. These liquid and vapor densities are then used to calculate the liquid and vapor fugacities f^L and f^V. A new estimate of the vapor pressure is then obtained by

multiplying the initial estimate of P_s by the ratio f^L/f^V. This procedure is continued iteratively until Equation V-10 is satisfied within a specified tolerance or $|1 - f^L/f^V|$ approaches a specified small value (e.g., 0.001). The final pressure is the calculated vapor pressure.

Mixture Thermodynamic Properties

The method for calculating mixture thermodynamic properties, such as density, enthalpy departure and entropy departure is virtually identical to the pure component method described above. The only difference is that mixture parameters (Equations (II-38)-(II-48)) rather than pure component parameters are used in the equation of state. Molar enthalpies for ideal gas mixtures must be calculated as mole fraction weighted averages of the component ideal gas molar enthalpies. The expression for molar entropy of ideal gas mixtures must include the entropy of mixing in addition to mole fraction weighted average of the component ideal gas molar entropies.

$$H^o \Sigma x_i M_i = \Sigma x_i H_i^o M_i \qquad \text{(V-11)}$$

$$S^o \Sigma x_i M_i = \Sigma x_i S_i^o M_i - R \Sigma x_i \ln x_i \qquad \text{(V-12)}$$

In Equations V-11 and V-12, H^o and H_i^o have the units Btu/lb and S^o and S_i^o have the unit Btu/lb ^oR; and H^o and S^o are the ideal gas mixture enthalpy and entropy, while H_i^o and S_i^o are the ideal gas enthalpy and entropy of the pure i^{th} component. The mixture average molecular weight is the sum of the products of mole fractions, x_i, and the component molecular weights, M_i.

Vapor-Liquid Equilibrium Prediction

Mixture vapor-liquid equilibrium predictions are more complicated than pure component vapor-liquid equilibrium predictions. However, mixture calculations can be carried out easily by computer.

The following condition equations for mixture vapor-liquid equilibrium can be derived from classical thermodynamics,

$$T^V = T^L \tag{V-13}$$

$$P^V = P^L \tag{V-14}$$

$$\bar{f}_i^V = \bar{f}_i^L \tag{V-15}$$

where the superscripts V and L refer to the vapor and liquid phases, respectively. To satisfy these condition equations it is necessary to calculate the fugacity of the i^{th} component, $\bar{f}_i$, in both vapor and liquid phases.

The fugacity of the i^{th} component in a fluid mixture, $\bar{f}_i$, is related to the equation of state by the following relation

$$RT \ln \left[\frac{\bar{f}_i/x_i}{\rho RT}\right] = \int_0^\rho \left[\rho \left(\frac{\partial PV}{\partial n_i}\right)_{T,V,n_{j\neq i}} - \rho RT\right] \frac{d\rho}{\rho^2} \tag{V-16}$$

In Equation V-16, x_i is the mole fraction of the i^{th} component in the mixture, which may be either liquid or vapor, V is the volume of the phase. When the mixture equation of state is used in Equation V-16, the expression for component fugacity given below results. .

$$RT\ln\bar{f}_i = RT\ln(\rho RTx_i) + \rho(B_o+B_{o_i})RT$$

$$+ 2\rho \sum_{j=1}^{n} x_j\left[-(A_oA_{o_i})^{\frac{1}{2}}(1-k_{ij}) - \frac{(C_oC_{o_i})^{\frac{1}{2}}}{T^2}(1-k_{ij})^3\right.$$

$$\left. + \frac{(D_oD_{o_i})^{\frac{1}{2}}}{T^3}(1-k_{ij})^4 - \frac{(E_oE_{o_i})^{\frac{1}{2}}}{T^4}(1-k_{ij})^5\right]$$

$$+\frac{\rho^2}{2}\left[3(b^2b_i)^{1/3}\,RT - 3(a^2a_i)^{1/3} - \frac{3(d^2d_i)^{1/3}}{T}\right]$$

$$+\frac{\alpha\rho^5}{5}\left[3(a^2a_i)^{1/3} + \frac{3(d^2d_i)^{1/3}}{T}\right]$$

$$+\frac{3\rho^5}{5}\left(a+\frac{d}{T}\right)(\alpha^2\alpha_i)^{1/3} \qquad \text{(V-17)}$$

$$+\frac{3(c^2c_i)^{1/3}\rho^2}{T^2}\left[\frac{1-\exp(-\gamma\rho^2)}{\gamma\rho^2} - \frac{\exp(-\gamma\rho^2)}{2}\right]$$

$$-\frac{2c}{\gamma T^2}\left(\frac{\gamma_i}{\gamma}\right)^{\frac{1}{2}}\left\{1-\exp(-\gamma\rho^2)\left[1+\gamma\rho^2+\frac{1}{2}\gamma^2\rho^4\right]\right\}$$

In Equation V-17, x_i is the mole fraction of the i^{th} component in the vapor phase if $\bar{f}_i^V$ is calculated; x_i is the mole fraction of the i^{th} component in the liquid phase if $\bar{f}_i^L$ is calculated.

All normally encountered types of mixture vapor-liquid equilibrium predictions can be carried out by searching for the appropriate value of V in the following relation

$$F(T,P,V) = \sum_{i=1} \frac{z_i(1-K_i)}{K_iV + (1-V)} \qquad \text{(V-18)}$$

In this relation z_i is the mole fraction of the i^{th} component in the feed mixture. At vapor-liquid equilibrium, one lb-mole of the feed mixture splits into V lb-moles of vapor and (1-V)=L lb-moles of liquid. The equilibrium vaporization ratio or K-value for the i^{th} component, K_i, is the ratio of y_i and x_i, the equilibrium mole fractions of the i^{th} component in the vapor and liquid phases respectively,

$$K_i = \left(\frac{y_i}{x_i}\right)_{\text{equilibrium}} \qquad \text{(V-19)}$$

For one lb-mole of feed mixture, the number of lb-moles of the i^{th} component in the feed, vapor and liquid are z_i, y_iV and $x_i(1-V)$, respectively, that is

$$z_i = y_i V + x_i (1-V) \qquad \text{(V-20)}$$

When z_i, K_i and V have been determined y_i and x_i can be solved for using Equations V-19 and V-20.

In virtually all vapor-liquid equilibrium predictions, two of the three quantities, T, P and V, are specified and the third is searched for. In the so-called flash calculation, T and P are specified and V is sought. In dew point calculations, V = 1 is specified and either P or T is sought. Similarly, in bubble point calculations, V = 0 is specified and P or T is sought. Other problems may specify values of V between 0 and 1. In all cases, the solution for the unknown (whether T, P or V) is that value of the unknown for which F(T,P,V) = 0 in Equation V-18. Trial-and-error search methods, including the Newton-Raphson method are applicable.

When the equation of state method is used for mixture vapor-liquid equilibrium predictions, the condition equation $\bar{f}_i^V = \bar{f}_i^L$, imposes an additional requirement which must be satisfied. The method for satisfying Equation V-15 for the case of a flash calculation (T and P specified) is shown in Figure V-1. Other types of calculations, such as dew and bubble point calculations, can be performed using analogous procedures. The first step in the procedure in Figure V-1 is to perform a flash calculation for the feed mixture composition using first estimates of the K-values, denoted by R_i. So-called ideal K-values (the ratio of vapor pressure to system pressure) are conveniently used as first estimates for the ratios R_i. The flash calculation yields the vapor-liquid split (V and L) and the component mole fractions, y_i for the vapor phase and x_i for the liquid phase. This allows calculation of the densities of the vapor ($\rho = d_V$) and liquid ($\rho = d_L$) phases using the equation of state.

The compositions and densities are then used to calculate component fugacities in each phase, using Equation V-17. If the vapor fugacity of any component is different from its liquid fugacity, the ratio R_i in Equation V-21 can be used as a new estimate for the K-value of the i^{th} component in a new flash calculation,

$$R_i = \frac{\bar{f}_i^L / x_i}{\bar{f}_i^V / y_i} \qquad \text{(V-21)}$$

This cycle is repeated until the thermodynamic condition for equilibrium (equality of component fugacities in each phase) is satisfied, for then R_i in Equation V-21 equals the equilibrium ratio, K_i in Equation V-19. By this method, with the convergence criterion $1 - \bar{f}_i^L / \bar{f}_i^V < 0.00001$, $i = 1,2,$ --- n, convergence usually is obtained within five iterations using the new equation of state.

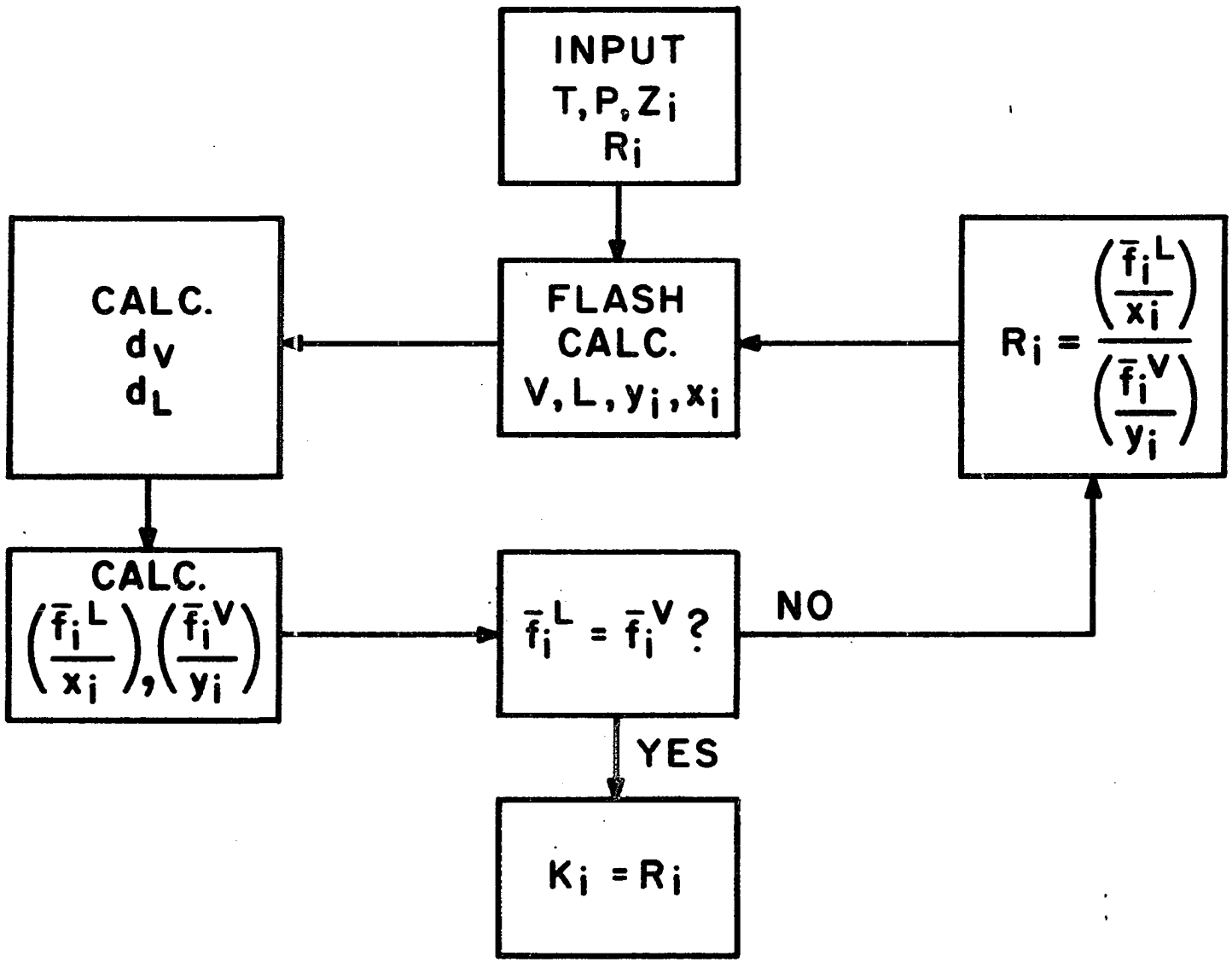

Figure V-1 ITERATIVE FLASH CALCULATION

CHAPTER VI

EVALUATIONS OF PREDICTIONS OF FLUID THERMODYNAMIC BEHAVIOR USING THE GENERALIZED CORRELATION

Predicted thermodynamic properties and K-values are compared with experimental data for broad ranges of systems and conditions to prove the generalized equation of state correlation is capable of describing virtually all conditions encountered industrially. The results of these comparisons are presented here for pure component properties, the mixture properties density, enthalpy and entropy and mixture vapor-liquid equilibria.

Pure Component Property Comparisons

Table VI-1 summarizes the results of using the generalized correlation for predicting the thermodynamic behavior of twenty-six pure fluids. These fluids include polar and nonpolar compounds, paraffin, olefin, naphthene and aromatic hydrocarbons and nonhydrocarbons. Densities are predicted with an average absolute deviation from experimental values of 1.53% for 1147 data points. Enthalpy departures are predicted with an average absolute deviation from experimental values of 1.74 Btu/lb for 620 data points. Vapor pressure also is predicted quite accurately, since saturated liquid fugacities along the vapor pressure curve are predicted with an average absolute deviation from saturated vapor fugacities of 1.08% for 663 points.

TABLE VI-1

PREDICTION OF PURE FLUID THERMODYNAMIC PROPERTIES USING GENERALIZED EQUATION OF STATE

(ρ = density, $H-H^{o}$ = enthalpy departure, f = fugacity at vapor pressure)

Fluid	Property	References	No. Data Pts.	Temp. Range °F	Pressure Range psia	Abs. Dev., Avg.*
Methane	ρ	26,108,109,	41	-253~662	129~2325	1.01
	$H-H^{o}$	44,116	35	-250~50	250~2000	1.59
	f	70	29	-259~(-116)	14.7~669	0.81
Ethane	ρ	14,90	50	-250~310	14.7~10000	1.22
	$H-H^{o}$	78,91	42	-258~310	249~3000	2.34
	f	14,90	38	-220~90	0.27~709	1.52
Propane	ρ	40,90,91	41	-250~527	14.7~3910	1.40
	$H-H^{o}$	116	37	-250~250	500~2000	1.33
	f	14,90,105	39	-260~206	0.001~617	1.43
n-Butane	ρ	90,91	41	-220~430	41.7~7000	0.53
	$H-H^{o}$	91	39	100~430	200~5000	1.43
	f	14,90	39	-110~305	0.18~550	0.62
n-Pentane	ρ	90,91	41	-200~460	14.7~10000	0.55
	$H-H^{o}$	91	39	100~460	200~10000	1.12
	f	14,90	37	-50~386	0.27~489	0.71
n-Hexane	ρ	90,101	41	-140~340	14.7~4000	0.42
	f	14,90	40	-10~454	0.22~439	0.75
n-Heptane	ρ	90,103	41	-90~460	14.7~3100	0.51
	$H-H^{o}$	35	17	512~706	79~2363	0.97
	f	90,47	29	70~497	0.73~350	0.72

TABLE VI-1 (Continued)

Fluid	Property	References	No. Data Pts.	Temp. Range °F	Pressure Range psia	Abs. Dev., Avg.*
n-Octane	ρ	90,30	54	-70~510	14.7~240	0.99
	$H-H^{o}$	60,74	70	75~600	200~1400	2.55
	f	74,90	50	70~560	0.22~350	1.15
n-Nonane	f	90	15	100~355	0.18~30	0.86
n-Decane	ρ	91	32	100~460	200~6000	1.47
	f	90	19	135~400	0.19~30	0.84
n-Undecane	f	90	19	165~440	0.18~30	1.36
i-Butane	ρ	90,91	73	-110~480	14.7~3000	1.74
	f	90,105	28	-136~275	0.1~394	2.52
i-Pentane	ρ	26,90,94	41	-60~392	14.7~882	1.49
	f	3,90	31	-122~370	0.01~394	1.47
Ethylene	ρ	14,72,90	41	-250~260	14.7~2000	2.63
	$H-H^{o}$	14	38	-120~260	100~2000	1.91
	f	14,90,105	35	-220~49	0.88~742	0.96
Propylene	ρ	14,29,73,90	61	-50~450	14.7~2940	2.0
	f	14,90,105	28	-195~197	0.04~670	1.72
Cyclohexane	ρ	77	26	60~536	1.2~592	1.45
	$H-H^{o}$	59	113	300~680	200~1400	2.20
	f	77,90	48	50~520	0.92~530	0.95
Benzene	ρ	76	65	464~644	375~923	1.75
	f	76,90	37	45~553	0.76~715	1.19
Toluene	$H-H^{o}$	115	103	50~650	50~2500	2.89
	f	90	26	45~280	0.2~30	0.96

TABLE VI-1 (Continued)

Fluid	Property	References	No. Data Pts.	Temp. °F Range	Pressure Range psia	Abs. Dev., Avg.*
Nitrogen	ρ	14,102	41	-321~240	14.7~9000	0.52
	$H-H^o$	66	48	-250~50	200~2000	0.35
	f	33	19	-309~-233	29~492	1.07
Hydrogen sulfide	ρ	63,82	41	40~340	100~2000	2.33
	f	48,111	24	-76~212	14.7~1306	0.68
Carbon dioxide	ρ	24	41	-22~284	294~5580	1.00
	$H-H^o$	24	39	-22~284	441~7350	2.23
	f	14	33	-70~88	75~1070	0.29
Nitrous oxide	ρ	20,69	126	-22~302	88~3233	1.83
Nitric oxide	ρ	75	33	-80~220	14.7~2000	2.77
Sulfur dioxide	ρ	109,110	62	-60~482	1.5~4408	1.88
Methyl chloride	ρ	61,111	60	-80~437	2.0~4408	2.98
Ethylene oxide	ρ	113	54	70~370	22~936	3.29

*Deviation functions are: $\frac{f^V - f^L}{f^V} \times 100\%$ at vapor pressure for data temperature %.

$$\frac{\rho_{exp} - \rho_{calc}}{\rho_{exp}} \times 100\%$$

$$(H-H^o)_{exp} - (H-H^o)_{calc}, \text{ Btu/lb.}$$

The consistent accuracy of predictions for wide classes of fluids (Table VI-1) indicates that the properties of other fluids can be predicted with confidence. In addition, the equation of state is thermodynamically consistent, since density, enthalpy and vapor pressure are predicted accurately. Thus, entropy, heat capacity and other thermodynamic properties can be predicted with confidence of accuracy. The results are conclusive, since over 2,400 data points are compared, the ranges of conditions are large and the fluids considered have wide variations in characteristics.

Mixture Property Comparisons

In all mixture comparison calculations, the generalized correlation has been adhered to faithfully. Predicted mixture densities, enthalpies and entropies are compared with experimental or derived data for 38 mixtures at more than 1,400 data points. The mixtures considered include natural gas, LPG and LNG mixtures containing as many as 10 components. For mixtures such as light naphthas and lean oils, whose compositions are defined in terms of hydrocarbon fractions rather than specific components, the characterization parameters T_{ci}, ρ_{ci} and ω_i must be determined from the available characteristics reported for the mixture. Methods for estimating these characterization parameters for hydrocarbon fractions encountered with light naphthas and lean oils will be discussed in Chapter VII.

Mixture Density Comparisons

Table VI-2 summarizes the results of using the generalized equation of state for density predictions for fourteen mixtures at temperatures from

TABLE VI-2

PREDICTION OF MIXTURE DENSITIES USING GENERALIZED EQUATION OF STATE

System Composition, Mole %	Ref.	Data points	Temperature, °F Min.	Temperature, °F Max.	Max press., psia	Abs. Dev. Avg. %
75.3% CH_4-24.7% C_3H_8	41	24	-238	32	5,000	1.06
50.0% CH_4-50.0% C_3H_8	41	27	-184	32	5,000	2.31
22.1% CH_4-77.9% C_3H_8	41	25	-184	32	5,000	0.86
80.0% C_3H_8- 20.0% C_6H_6	91	6	100	220	1,500	1.78
60.0% C_3H_8-40.0% C_6H_6	91	6	100	220	1,500	0.95
40.0% C_3H_8-60.0% C_6H_6	91	6	100	220	1,500	0.73
20.0% C_3H_8-80.0% C_6H_6	91	6	100	220	1,500	0.95
5.3% CH_4-47.3% C_4H_{10} -47.4% $C_{10}H_{22}$	91	5	100	460	4,000	0.99
7.7% CH_4-23.1% C_4H_{10} -69.2% $C_{10}H_{22}$	91	4	100	460	4,000	2.58
7.7% CH_4-69.2% C_4H_{10} -23.1% $C_{10}H_{22}$	91	5	100	460	4,000	1.25
20.0% CH_4-60.0% C_4H_{10} -20.0% $C_{10}H_{22}$	91	4	100	460	4,000	0.52
LNG Mixture No. 1*	54	4	-283	-256	14.7	0.96
LNG Mixture No. 2*	54	4	-283	-256	14.7	0.80
LNG Mixture No. 3*	54	4	-283	-256	14.7	0.53

*LNG Mixture No. 1: 4.2% N_2-88.3% CH_4-4.7% C_2H_6-1.4% C_3H_8-1.3% C_4H_{10}

*LNG Mixture No. 2: 5.7% N_2-87.6% CH_4-3.0% C_2H_6-2.0% C_3H_8-1.8% C_4H_{10}

*LNG Mixture No. 3: 4.8% N_2-84.8% CH_4-7.8% C_2H_6-1.8% C_3H_8-0.8% C_4H_{10}

-283°F to 460°F and pressures from 14.7 psia to 5000 psia. The average absolute deviation of predicted densities from experimental values is 1.16%. This deviation is within twice the reported experimental uncertainty for most of the mixtures studied. These results indicate that for many situations, the generalized equation of state can quite adequately predict densities of industrial mixtures, including LNG and LPG.

Mixture Enthalpy Comparisons

Table VI-3 summarizes the results of using the generalized equation of state for enthalpy departure predictions for twenty-four mixtures at temperatures from -250°F to 680°F and pressures from 50 psia to 2500 psia. The average absolute deviation of predicted enthalpy departures from experimental values is 2.20 Btu/lb, which is within three times the experimental uncertainty for most of the mixtures studied. Many different types of mixtures are included in Table VI-3, including not only mixtures having the characteristics of LPG, but a ten component natural gas-LNG mixture and a fifteen component rich absorber oil mixture. The accurate predictions of enthalpy for these widely varying mixtures show the generalized equation of state can be used for enthalpy predictions needed in many situations in the natural gas and petroleum processing industries.

Mixture Entropy Comparisons

The ability of the generalized equation of state to predict mixture entropies was tested using entropy values presented by Bhirud and Powers[6] for a nominal 94.8 mole percent methane and 5.2 mole percent propane mixture. Sixty-two points were compared, covering a temperature range from -250°F to 300°F and a pressure range from 250 psia to 2000 psia. The

TABLE VI-3

PREDICTION OF MIXTURE ENTHALPIES USING GENERALIZED EQUATION OF STATE

System Composition, Mole %	Ref.	Data points	Temperature, °F Min.	Temperature, °F Max.	Max. press., psia	Abs. Dev. Avg. Btu/lb
43.4% N_2-56.6% CH_4	68	54	-250	250	2,000	1.03
94.8% CH_4-5.2% C_3H_8	6,67	25	-250	250	2,000	1.31
88.3% CH_4-11.7% C_3H_8	68	47	-250	250	2,000	1.44
72.0% CH_4-28.0% C_3H_8	68	45	-250	250	2,000	2.25
49.4% CH_4-50.6% C_3H_8	116	45	-250	250	2,000	3.48
23.4% CH_4-76.6% C_3H_8	116	50	-250	250	2,000	2.74
76.3% C_2H_6-23.7% C_3H_8	78	29	-240	240	2,000	1.80
49.8% C_2H_6-50.2% C_3H_8	78	28	-240	240	2,000	1.37
27.6% C_2H_6-72.4% C_3H_8	78	17	-240	240	2,000	1.92
36.6% CH_4-31.1% C_2H_6 -32.3% C_3H_8	34	31	-240	240	2,000	1.74
79.3% C_5H_{12}-20.7% C_6H_{12}	59	115	280	680	1,400	1.15
61.2% C_5H_{12}-38.8% C_6H_{12}	59	118	280	680	1,400	1.40
38.5% C_5H_{12}-61.5% C_6H_{12}	59	112	300	680	1,400	1.17
19.7% C_5H_{12}-80.3% C_6H_{12}	59	103	400	680	1,400	3.91
80.9% C_5H_{12}-19.1% C_8H_{18}	60	66	75	600	1,400	3.36
59.7% C_5H_{12}-40.3% C_8H_{18}	60	66	75	600	1,400	3.59
39.2% C_5H_{12}-60.8% C_8H_{18}	60	47	75	600	1,400	4.32
21.8% C_5H_{12}-78.2% C_8H_{18}	60	60	75	600	1,400	3.03
50.0% CH_4-50.0% Toluene	115	44	-100	600	2,500	2.04
20.0% C_5H_{12}-20.2% C_6H_{12} -59.8% Benzene	61	43	380	600	1,400	2.26
33.3% C_5H_{12}-33.4% C_6H_{12} -33.3% Benzene	61	40	340	600	1,400	2.35
60.1% C_5H_{12}-20.0% C_6H_{12} -19.9% Benzene	61	59	320	600	1,400	2.32

TABLE VI-3 (Continued)

System Composition, Mole %	Ref.	Data points	Temperature, °F Min.	Temperature, °F Max.	Max. press., psia	Abs. Dev. Avg. Btu/lb
Natural gas-LNG mixture*	36	12	-200	200	1,000	1.66**
Rich Absorber Oil	61	68	-100	600	2,500	3.3

*Nat. gas-LNG mixture composition:
0.6% N_2 - 95.79% CH_4 - 3.0% C_2H_6 - 0.39% C_3H_8
- 0.07 % iC_4H_{10} - 0.07% C_4H_{10} - 0.03% iC_5H_{12}
- 0.01% C_5H_{12} - 0.025% 3-methyl pentane
- 0.015% 2-methylhexane.

**Isobaric enthalpy difference data were used. The deviation function for this case is $(H_2-H_1)_{exp} - (H_2-H_1)_{calc}$ where 1 and 2 are inlet and outlet conditions in calorimeter.

average absolute deviation of predicted entropy departures from the reported values was 0.0042 Btu/lb-^{o}R. The results of this study show the generalized equation of state can be used for accurate predictions of entropies for both gas and liquid mixtures.

Mixture K-value Comparisons

Conditions for mixture K-value comparisons are summarized in Table VI-4. Because of the well-known problem of evaluating the accuracy of experimental K-value data, average absolute deviations for K-values are not reported in Table VI-4. Instead, direct comparisons of experimental and calculated phase compositions and K-values for numerous systems are shown either graphically or numerically, in Figures (VI-1)-(VI-13) and Tables (VI-5)-(VI-10). Inspection of these comparisons of predicted and experimental phase compositions and K-values shows that not only the magnitudes but trends of the predicted phase compositions are in good agreement with experimental results. For most points, the generalized correlation predicts phase compositions within the larger of 5% or 0.0005 of experimental mole fractions. For convenience of presentation, the results are discussed for particular types of interactions. The interaction types included are: (1) nonhydrocarbon-nonhydrocarbon, (2) nonhydrocarbon-hydrocarbon, (3) paraffin-paraffin, (4) paraffin-naphthene, and (5) paraffin-aromatic.

Nonhydrocarbon-nonhydrocarbon interactions in natural gas systems occur principally between nitrogen, carbon dioxide and hydrogen sulfide. Figure VI-1 compares predicted vapor and liquid compositions with experimental data for the carbon dioxide-hydrogen sulfide system. The generalized correlation predicts phase compositions in agreement with experimental behavior over the temperature range from 40^{o}F to 200^{o}F at pressures from 588 psia to 1176 psia.

TABLE VI-4

PHASE EQUILIBRIUM DATA USED FOR EVALUATION OF GENERALIZED CORRELATION

System components	Ref.	Lowest temp. (°F)	Highest temp. (°F)	Highest pressure psia
CH_4-C_2H_6	112	-200	-100	740
CH_4-C_3H_8	79,112	-200	50	1100
CH_4-C_6H_{14}	53	-58	212	1470
CH_4-C_7H_{16}	17,51	-60	40	1000
CH_4-C_8H_{18}	52	-58	212	1029
CH_4-$C_{10}H_{22}$	91	40	280	3000
CH_4-Toluene	16	-60	0	1500
CH_4-Methyl Cyclohexane	15	-60	0	1500
C_2H_6-C_5H_{12}	86	40	160	900
C_2H_6-C_7H_{16}	71	250	250	800
C_2H_6-$C_{10}H_{22}$	85	40	160	400
C_3H_8-C_5H_{12}	92	220	220	300
C_3H_8-$C_{10}H_{22}$	88	40	280	300
C_3H_8-Benzene	91	100	220	500
C_4H_{10}-C_7H_{16}	49	200	350	200
C_4H_{10}-$C_{10}H_{22}$	87	100	220	200
N_2-CH_4	9	-238	-180	500
N_2-C_2H_6	27	-140	-180	700
N_2-C_4H_{10}	1	100	100	4020
N_2-C_5H_{12}	55	-200	0	4047
N_2-C_7H_{16}	1	90	175	4027
N_2-CO_2	117	-40	32	2015
CO_2-CH_4	25	-65	29	1000
CO_2-C_2H_6	55	-60	60	783
CO_2-C_3H_8	142,84	-40	160	900
CO_2-C_4H_{10}	84	100	220	900
CO_2-H_2S	7	23	176	1176

TABLE VI-4 (Continued)

System components	Ref.	Lowest temp. (°F)	Highest temp. (°F)	Highest pressure psia
H_2S-CH_4	50,83	0	160	1900
H_2S-C_3H_8	11	-68	160	400
H_2S-C_5H_{12}	93	40	160	700
H_2-C_2H_6	113	-100	0	2000
He-N_2	12	-320.7	-320.7	1000
CH_4-C_2H_6-C_3H_8	112	-150	-75	800
CH_4-C_2H_6-C_7H_{16}	107	-60	-40	1000
CH_4-C_3H_8-C_7H_{16}	107	-60	-20	1000
H_2-CH_4-C_2H_6	19	-200	-100	1000
N_2-CH_4-C_2H_6	19	-200	-100	1000
CH_4-C_2H_6-C_3H_8-C_4H_{10}	23	-60	-60	204
CH_4-C_2H_6-C_3H_8-C_4H_{10}-C_5H_{12}	23,37	-20	100	1736
CH_4-C_2H_6-C_3H_8-C_6H_{14}-C_7H_{16}-$C_{10}H_{22}$	106	150	250	3000
Natural Gas System (10 components)	36	-195	-120	500
Absorber System (15 components)	114	-40	40	1500

Thus, although the generalized correlation parameters were developed from normal paraffin hydrocarbon data, the correlation is sufficiently general and the mixing rules are adequate to predict nonhydrocarbon system behavior.

Nonhydrocarbon-hydrocarbon interactions occur in several of the systems studied. Direct comparisons of predicted and experimental phase compositions or K-values are made for several systems in Figures (VI-2)-(VI-5). For the methane-nitrogen system the temperature-composition diagram in Figure VI-2 shows that predicted compositions for both methane and nitrogen agree with experimental data down to temperatures as low as -240°F. In addition, enthalpies for the methane-nitrogen system also are predicted accurately. For the methane-hydrogen sulfide system, isotherms of K-values plotted versus pressure in Figure VI-3 show good agreement with experimental behavior. For the propane-carbon dioxide system, the plot of K-values versus pressure in Figure VI-4 for 40°F and 130°F indicates that K-values for this system are predicted quite accurately, even near the cricondenbar pressure. For the propane-hydrogen sulfide system, the temperature-composition plot in Figure VI-5 shows that predicted phase compositions are accurate for propane mole fractions greater than azeotrope compositions at pressures from 20 psia to 300 psia. From the direct comparisons for the above systems it can be concluded that the generalized equation adequately describes nonhydrocarbon-hydrocarbon interactions.

Paraffin-paraffin hydrocarbon interactions occur in a large number of the systems studied. Densities and enthalpies for these systems are both accurately predicted. Direct comparisons of predicted and experimental phase behavior for systems having only paraffin-paraffin interactions are made in Figures (VI-6)-(VI-9) and Tables (VI-5)-(VI-7). Based on the

expected uncertainties in the data, all of these comparisons indicate paraffin-paraffin hydrocarbon interactions are adequately described by the generalized correlation. The accuracy of predicted phase compositions for the methane-propane system can be realized from Figures VI-6 and VI-7, which, respectively, show pressure composition diagrams for temperatures above and below $0^{\circ}F$. For the full range of conditions, including temperatures down to $-200^{\circ}F$, predicted phase compositions and K-values are within a few standard deviations of the experimental values. The high accuracy of predicted phase compositions for the methane-ethane system can be seen in Figure VI-8, which shows pressure-composition diagrams for $-99.8^{\circ}F$ and $-150^{\circ}F$. A similar plot, Figure VI-9, for the ethane-normal pentane system at $160^{\circ}F$ shows good agreement between predicted and experimental phase compositions from 100 psia to 900 psia. Ternary system phase composition comparisons in Tables (VI-5)-(VI-7), for three systems, methane-ethane-propane, methane-ethane-normal heptane and methane-propane-normal heptane show the high accuracy of phase predictions.

Paraffin-naphthene hydrocarbon interactions can be studied directly utilizing enthalpy data for the normal pentane-cyclohexane system (k_{ij} = 0.00) and phase behavior data for the methane-methyl cyclohexane system (k_{ij} = 0.085). The average deviation of predicted enthalpies from the experimental values for four normal pentane-cyclohexane mixtures is 1.37 Btu/lb, which is less than the reported experimental uncertainty, indicating a very reasonable description of paraffin-naphthene interactions by the generalized correlation. Further, vapor-liquid equilibrium for the methane-methyl cyclohexane system is predicted accurately, since methane K-values are in good agreement with experimental data, as shown in Figure VI-10.

Paraffin-aromatic hydrocarbon interactions can be studied with respect to enthalpy and phase behavior for the methane-toluene system (k_{ij} = 0.135) and with respect to density and phase behavior for the propane-benzene system (k_{ij} = 0.02). The average absolute deviation of predicted enthalpies from experimental data for the methane-toluene system is 2.04 Btu/lb, indicating a good description of this system by the generalized correlation. Methane K-values also are predicted accurately, as shown in Figure VI-10. Densities are predicted with extreme accuracy for the propane-benzene system. The overall average deviation for densities of four propane-benzene mixtures is very low, 0.97%. For K-values, the plot in Figure VI-11 of phase equilibrium for the propane-benzene system shows that the generalized correlation provides an adequate representation of paraffin-aromatic hydrocarbon interactions.

In summary, it is obvious from the many tests which have been made, that the generalized equation of state correlation accurately predicts thermodynamic properties and vapor-liquid equilibrium for virtually all mixtures and conditions encountered in the hydrocarbon processing industry. No previous general correlation has been capable of accurate and self consistent predictions of all thermodynamic properties, including densities, enthalpies, entropies, vapor pressures and K-values for such wide classes of fluids over such wide ranges of conditions.

TABLE VI-5

COMPARISON OF PREDICTED AND EXPERIMENTAL PHASE COMPOSITIONS FOR THE METHANE-ETHANE-PROPANE SYSTEM

(Component Indices: 1=Methane, 2=Ethane, 3=Propane)

Component Index	Feed Mole %	Liquid Mole %		Vapor Mole %	
		Exptl.	Calc.	Exptl.	Calc.
(T = -150.0°F, P = 32.0 psia)					
1	44.48	7.15	7.74	81.80	81.77
2	47.50	77.01	76.57	17.99	17.99
3	8.02	15.84	15.69	0.21	0.24
(T = -150°F, P = 100.0 psia)					
1	60.49	23.59	25.46	97.39	97.52
2	13.24	24.16	23.69	2.32	2.20
3	26.27	52.25	50.86	0.29	0.28
(T = -150.0°F, P = 200.0 psia)					
1	76.19	54.87	54.59	97.51	97.64
2	20.36	38.26	38.53	2.46	2.32
3	3.45	6.87	6.88	0.03	0.04
(T = -150.0°F, P = 300.0 psia)					
1	92.60	85.65	82.35	99.55	99.54
2	2.49	4.62	5.63	0.35	0.36
3	4.91	9.73	12.02	0.10	0.10
(T = -75.0°F, P = 100.0 psia)					
1	44.95	8.13	8.45	81.76	81.96
2	16.56	20.52	20.53	12.61	12.54
3	38.49	71.35	71.02	5.63	5.49
(T = -75.0°F, P = 200.0 psia)					
1	54.07	17.77	17.91	90.36	90.59
2	12.39	18.34	18.36	6.45	6.37
3	33.54	63.89	63.73	3.19	3.04
(T = -75.0°F, P = 400.0 psia)					
1	61.99	37.25	36.35	86.73	87.10
2	32.31	51.93	52.67	12.70	12.38
3	5.70	10.82	10.98	0.57	0.53
(T = -75.0°F, P = 600.0 psia)					
1	74.34	58.26	55.16	90.42	90.70
2	21.65	34.27	36.75	9.03	8.77
3	4.01	7.47	8.09	0.55	0.53

TABLE VI-5 (Continued)

Component Index	Feed Mole %	Liquid Mole %		Vapor Mole %	
		Exptl.	Calc.	Exptl.	Calc.
(T = -75.0°F, P = 800.0 psia)					
1	84.50	78.40	74.96	90.60	90.60
2	14.76	20.37	23.57	9.14	9.12
3	0.74	1.23	1.47	0.25	0.28

TABLE VI-6

COMPARISON OF PREDICTED AND EXPERIMENTAL PHASE COMPOSITIONS FOR THE METHANE-ETHANE-n-HEPTANE SYSTEM
(Component Indices: 1=Methane, 2=Ethane, 3= n-Heptane)

Component Index	Feed Mole %	Liquid Mole %		Vapor Mole %	
		Exptl.	Calc.	Exptl.	Calc.
(T = -40°F, P = 800 psia)					
1	66.28	38.00	36.77	94.65	94.25
2	10.87	16.30	16.29	5.44	5.74
3	22.85	45.70	46.94	0.00	0.01
(T = -60°F, P = 800 psia)					
1	69.28	44.00	40.84	95.56	93.97
2	12.57	19.70	20.11	5.44	6.02
3	18.15	36.30	39.05	0.00	0.01

TABLE VI-7

COMPARISON OF PREDICTED AND EXPERIMENTAL PHASE COMPOSITIONS FOR THE METHANE-PROPANE-n-HEPTANE SYSTEM

(Component Indices: 1=Methane, 2=Propane, 3 = n-Heptane)

Component Index	Feed Mole %	Liquid Mole %		Vapor Mole %	
		Exptl.	Calc.	Exptl.	Calc.
($T = -20^{\circ}F$, P = 600 psia)					
1	61.63	27.30	28.07	95.95	95.75
2	22.22	40.40	39.91	4.05	4.24
3	16.15	32.30	32.02	0.00	0.01
($T = -20^{\circ}F$, P = 1000 psia)					
1	70.22	42.60	39.29	97.84	97.69
2	9.68	17.20	18.01	2.16	2.28
3	20.10	40.20	42.70	0.00	0.03
($T = -60^{\circ}F$, P = 800 psia)					
1	72.42	45.90	43.73	98.94	98.86
2	8.33	15.60	16.14	1.06	1.13
3	19.25	38.50	40.13	0.00	0.01

TABLE VI-8

COMPARISON OF PREDICTED AND EXPERIMENTAL PHASE COMPOSITIONS FOR THE HYDROGEN-METHANE-ETHANE SYSTEM

(Component Indices: 1=Hydrogen, 2=Methane, 3=Ethane)

Component Index	Feed Mole %	Liquid Mole %		Vapor Mole %	
		Exptl.	Calc.	Exptl.	Calc.
($T = -100^{\circ}F$, $P = 500$ psia)					
1	23.78	1.33	1.28	46.23	46.17
2	37.64	29.42	28.81	45.86	46.42
3	38.58	69.25	69.91	7.91	7.41
($T = -100^{\circ}F$, $P = 1000$ psia)					
1	24.78	3.76	2.99	45.79	46.92
2	49.09	49.57	49.65	48.62	48.53
3	26.13	46.67	47.36	5.59	4.55
($T = -200^{\circ}F$, $P = 500$ psia)					
1	36.21	3.27	2.58	69.15	71.70
2	61.42	92.03	92.83	30.80	28.27
3	2.37	4.70	4.59	0.05	0.03

TABLE VI-9

COMPARISON OF PREDICTED AND EXPERIMENTAL PHASE COMPOSITIONS FOR A NATURAL GAS - LNG MIXTURE

(Component Indices: 1=Nitrogen, 2=Methane, 3=Ethane, 4=Propane, 5=Isobutane, 6 = n-Butane, 7=Isopentane, 8=n-Pentane, 9=3-Methylpentane, 10=2-Methylhexane)

Component Index	Feed Mole %	Liquid Mole %		Vapor Mole %	
		Exptl.	Calc.	Exptl.	Calc.
(T = -195.0°F, P = 100.0 psia)					
1	0.60	0.06	0.05	0.67	0.67
2	95.79	70.01	71.09	98.98	98.92
3	3.00	24.17	23.46	0.38	0.40
4	0.39	3.47	3.44	9×10^{-3}	3×10^{-3}
5	0.07	0.63	0.62	7×10^{-4}	7×10^{-5}
6	0.07	0.63	0.62	4×10^{-4}	3×10^{-5}
7	0.03	0.27	0.27	0.00	2×10^{-6}
8	0.01	0.09	0.09	0.00	4×10^{-7}
9	0.025	0.23	0.22	0.00	1×10^{-7}
10	0.015	0.14	0.13	0.00	2×10^{-8}
(T = -120.0°F, P = 498.5 psia)					
1	0.60	0.14	0.16	0.65	0.65
2	95.79	80.69	82.05	97.33	97.41
3	3.00	14.03	12.99	1.89	1.82
4	0.39	2.92	2.84	0.11	0.10
5	0.07	0.68	0.60	9×10^{-3}	8×10^{-3}
6	0.07	0.71	0.62	8×10^{-3}	6×10^{-3}
7	0.03	0.31	0.28	1×10^{-3}	1×10^{-3}
8	0.01	0.11	0.09	2×10^{-4}	3×10^{-4}
9	0.025	0.24	0.23	5×10^{-4}	3×10^{-4}
10	0.015	0.14	0.14	3×10^{-4}	1×10^{-4}

TABLE VI-10

COMPARISON OF PREDICTED AND EXPERIMENTAL PHASE COMPOSITIONS FOR A 103 MOLECULAR WEIGHT LEAN OIL ABSORBER SYSTEM AT -40°F AND 1000 psia

(Component Indices: 1=Nitrogen, 2=Carbon Dioxide, 3=Methane, 4=Ethane, 5=Propane, 6=i-Butane, 7=n-Butane, 8=i-Pentane, 9=n-Pentane, 10=n-Hexane, 11=n-Heptane, 12=n-Octane, 13=n-Nonane, 14=n-Decane, 15=n-Undecane)

Component Index	Feed Mole %	Liquid Mole %		Vapor Mole %	
		Exptl.	Calc.	Exptl.	Calc.
1	0.531	0.065	0.081	0.570	0.583
2	0.816	0.818	0.650	0.770	0.835
3	90.620	42.92	42.34	96.16	96.17
4	2.600	6.49	6.24	2.25	2.18
5	0.313	1.70	1.45	0.179	0.182
6	0.024	0.155	0.170	0.0073	0.0072
7	0.055	0.395	0.417	0.0110	0.0130
8	0.090	0.704	0.788	0.0084	0.0097
9	0.069	0.602	0.620	0.0051	0.0056
10	0.192	1.77	1.81	0.0058	0.0057
11	1.110	10.43	10.70	0.0090	0.0074
12	2.450	22.61	23.74	0.0160	0.0030
13	0.943	9.31	9.14	0.0041	0.0006
14	0.142	1.50	1.38	0.0001	38×10^{-5}
15	0.049	0.539	0.475	0.0000	46×10^{-6}

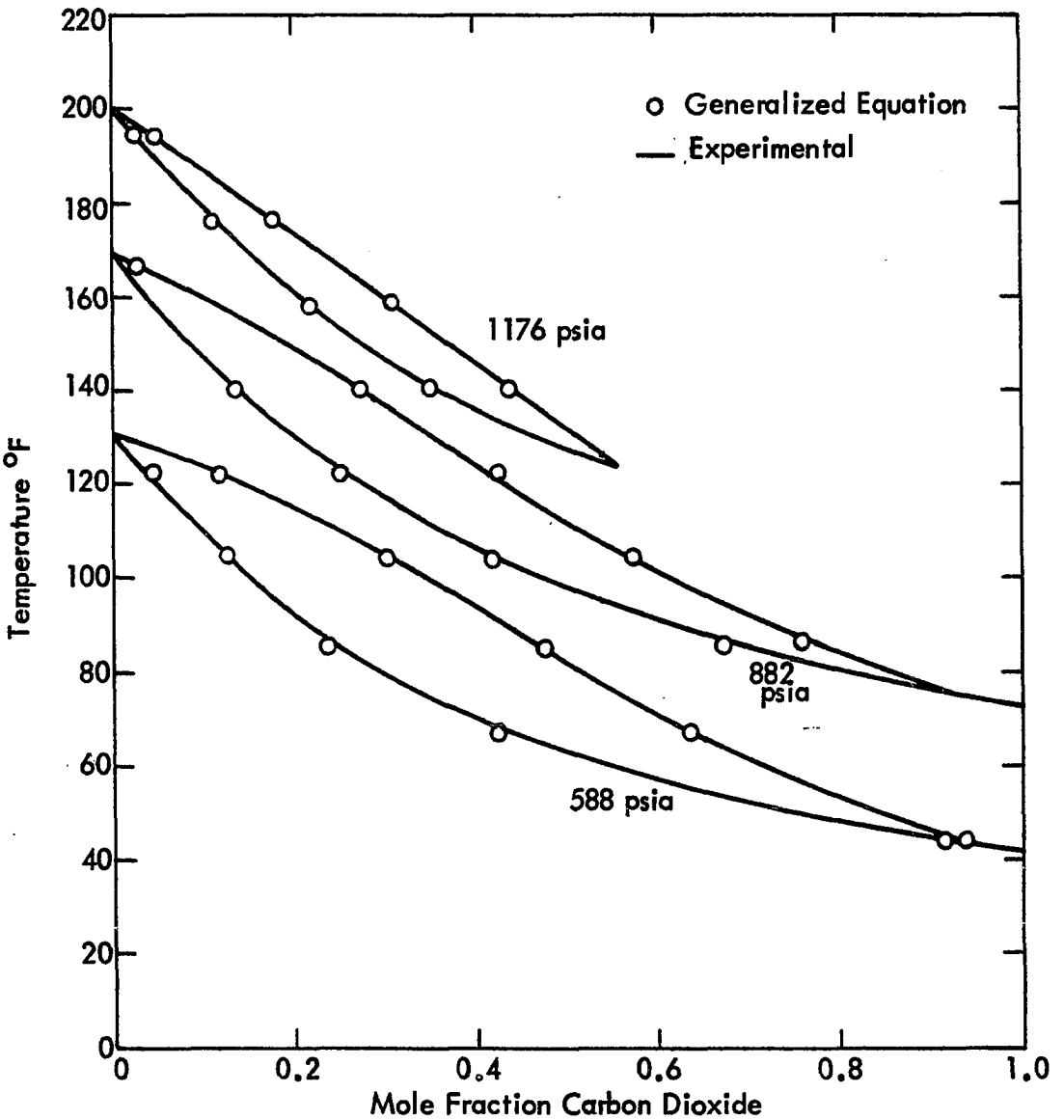

Figure VI-1. Comparison of Predicted and Experimental Phase Compositions for the Carbon Dioxide-Hydrogen Sulfide System at 1176 psia, 882 psia and 588 psia.

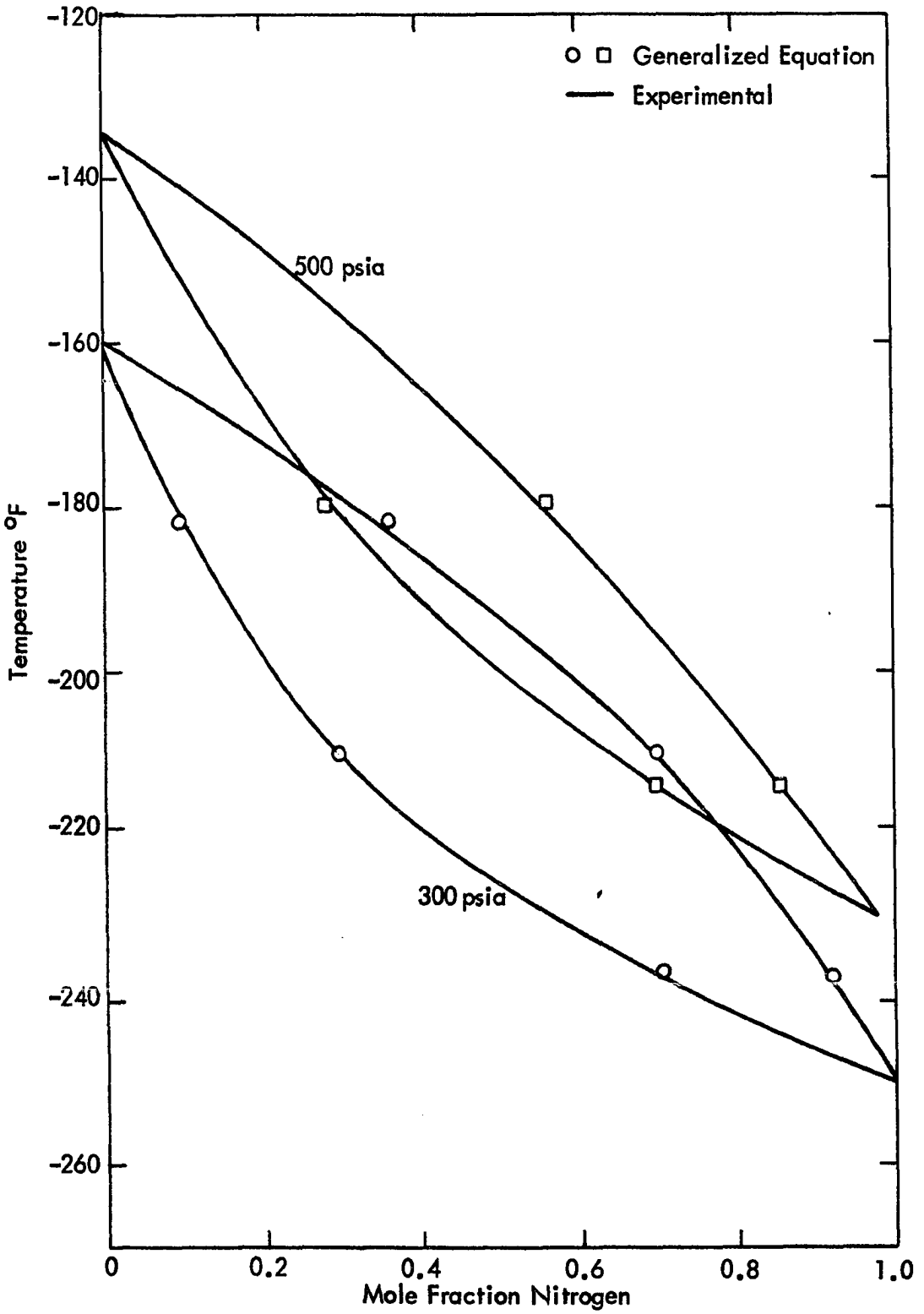

Figure VI-2 Comparison of Predicted and Experimental Phase Compositions for the Methane-Nitrogen System at 500 psia and 300 psia.

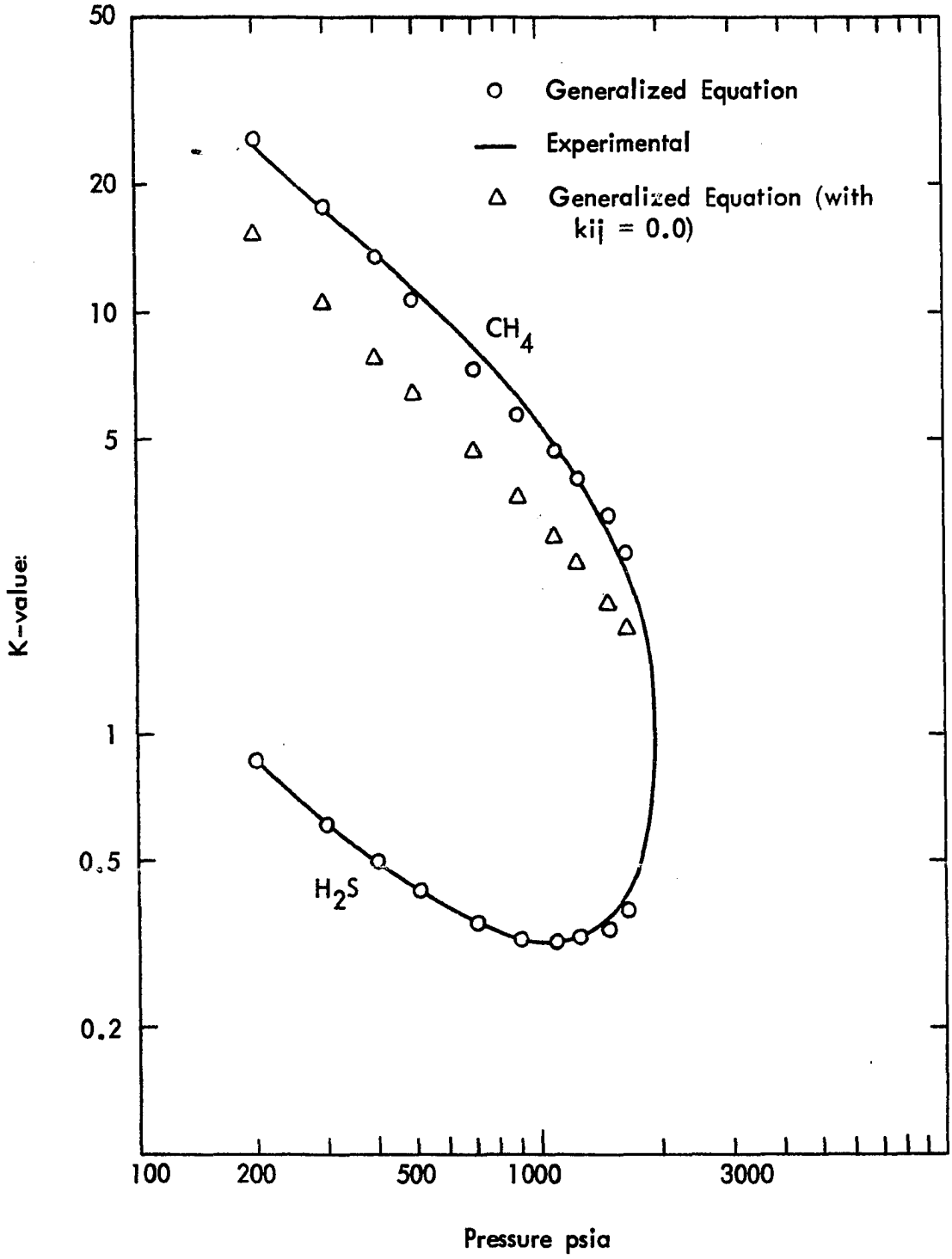

Figure VI-3 Comparison of Predicted and Experimental K-values for the Methane-Hydrogen Sulfide System at 40°F.

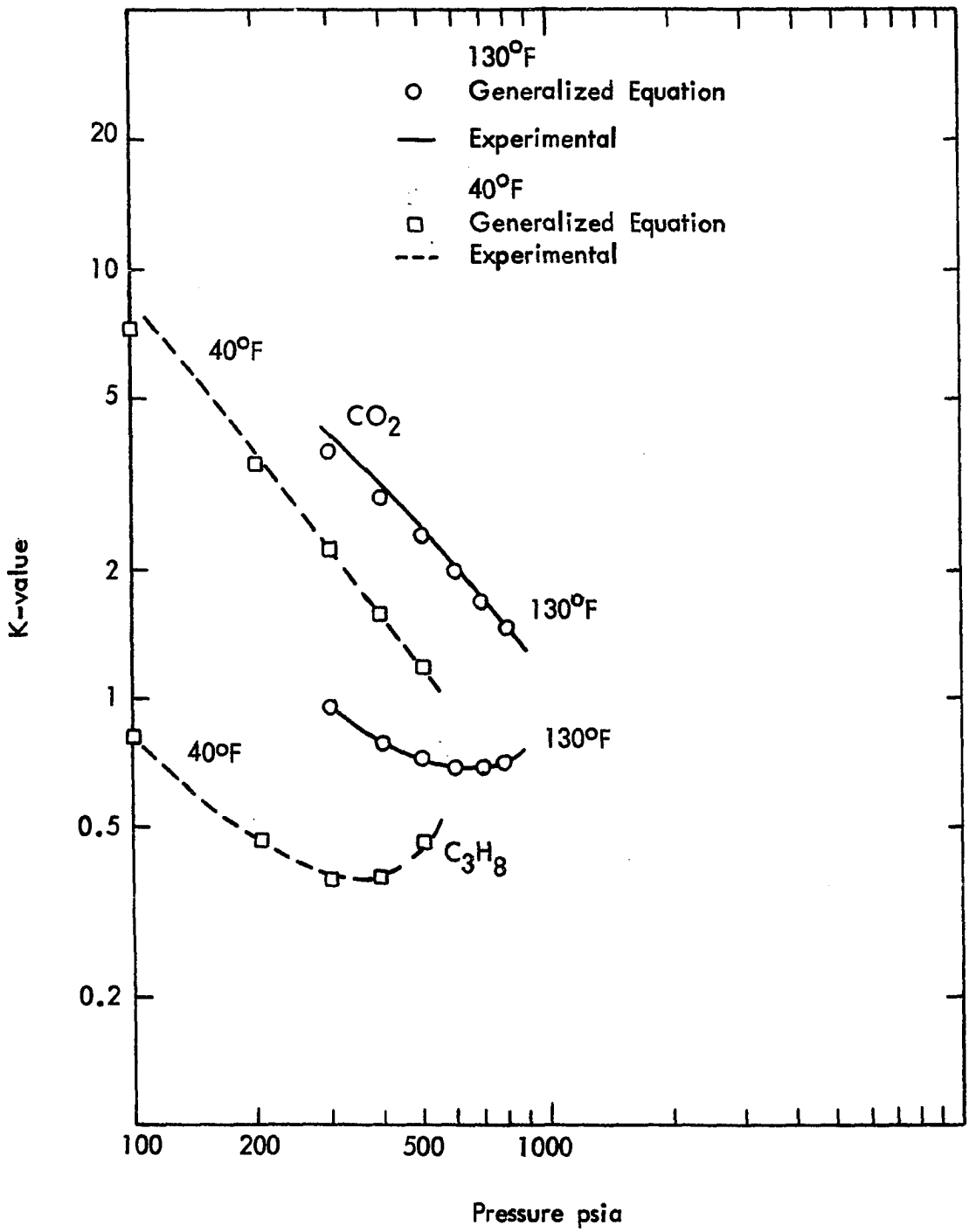

Figure VI-4 Comparison of Predicted and Experimental K-values for the Propane-Carbon Dioxide System at 40°F and 130°F.

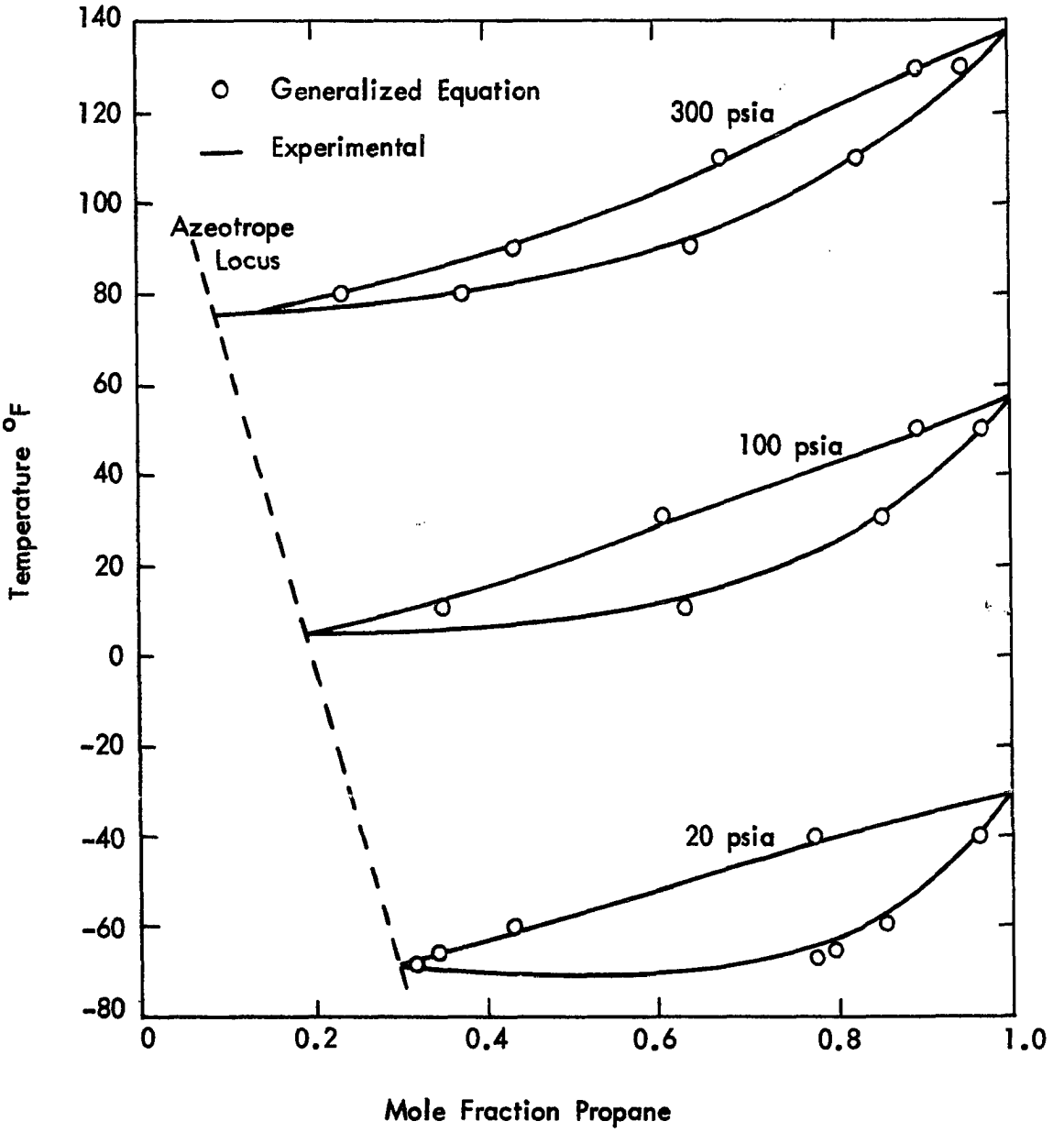

Figure VI-5 Comparison of Predicted and Experimental Phase Compositions for the Propane-Hydrogen Sulfide System at 20 psia, 100 psia and 300 psia.

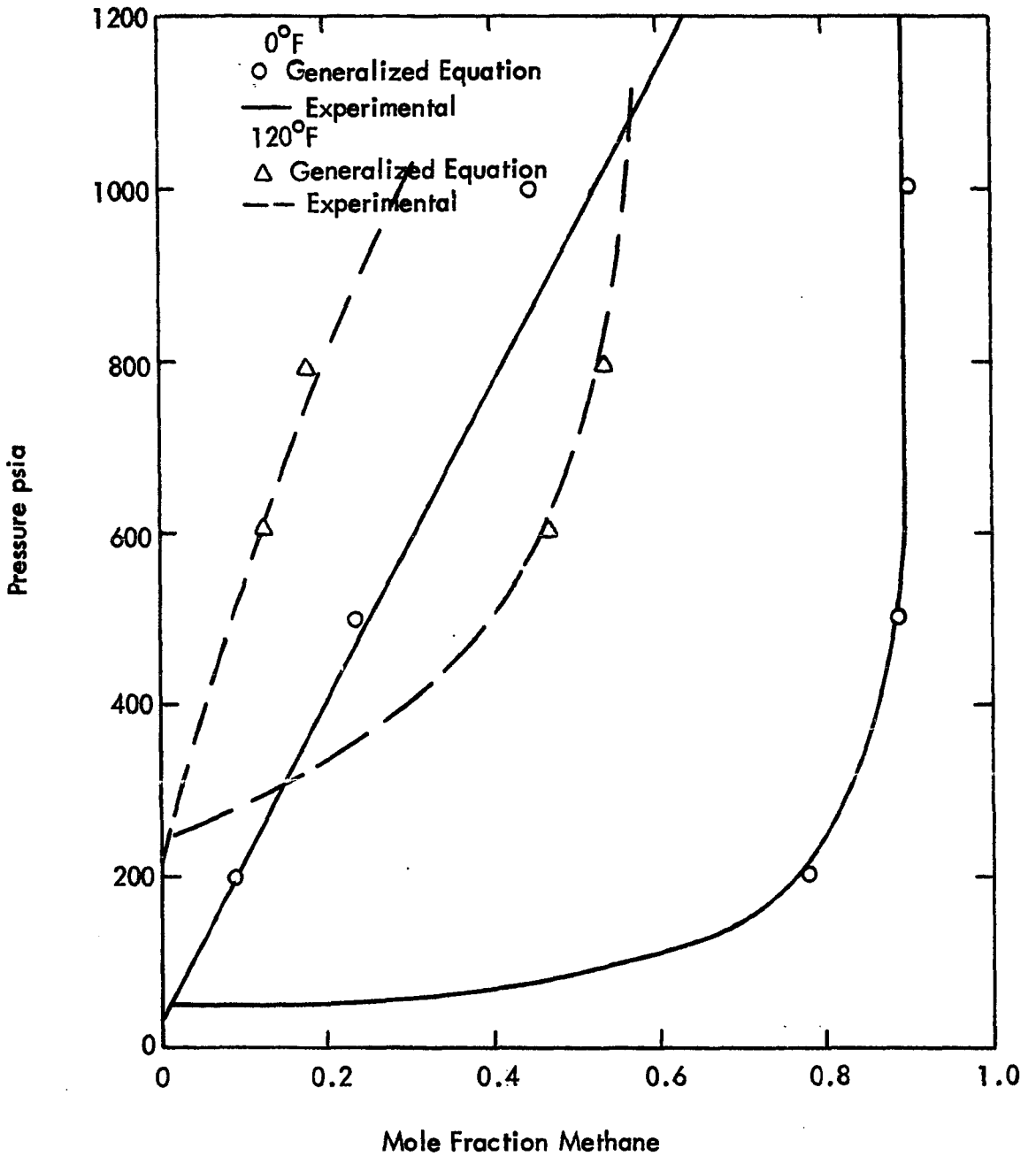

Figure VI-6 Comparison of Predicted and Experimental Phase Compositions for the Methane-Propane System at 0°F and 120°F.

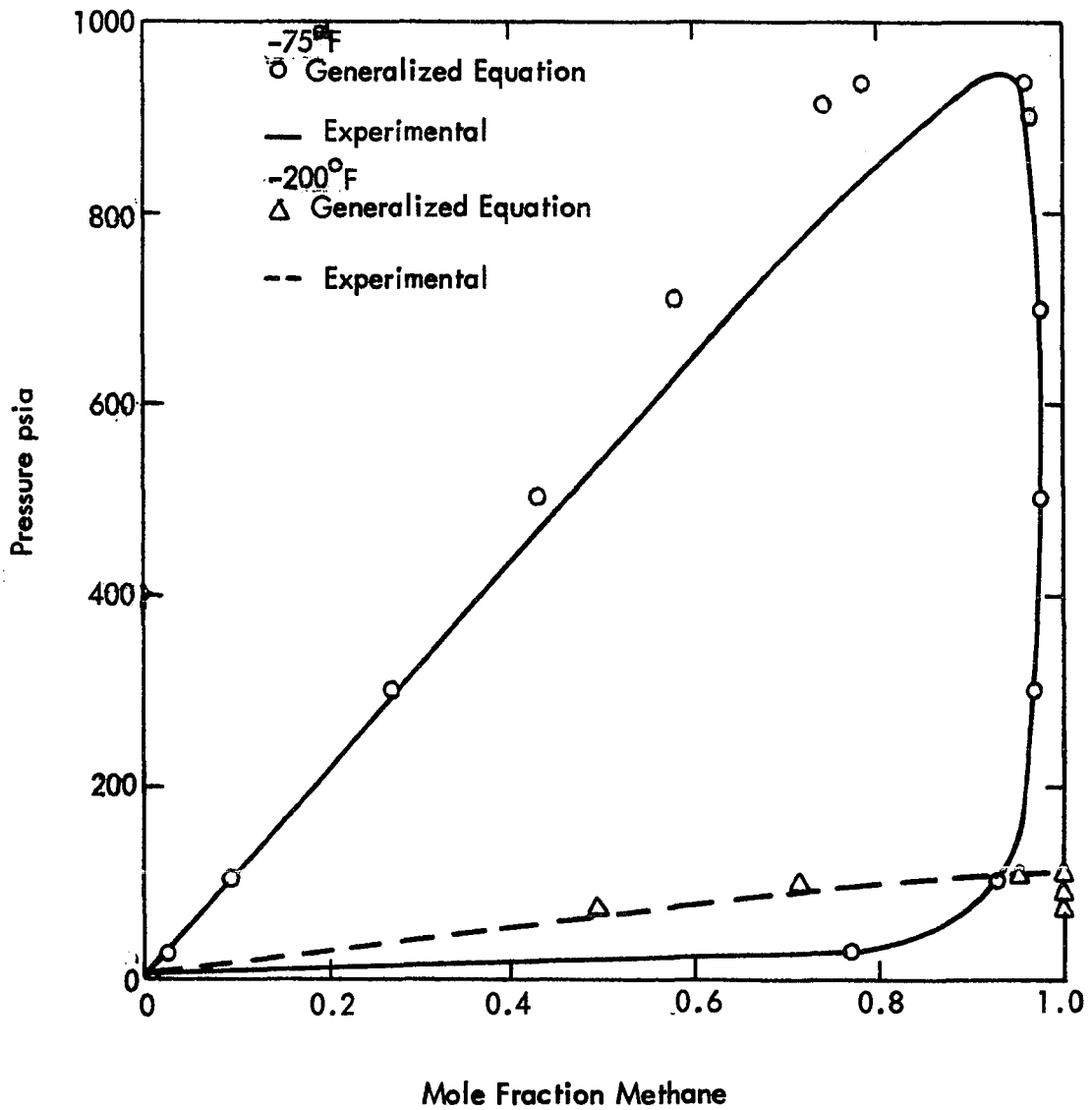

Figure VI-7 Comparison of Predicted and Experimental Phase Compositions for the Methane-Propane System at -75°F and -200°F.

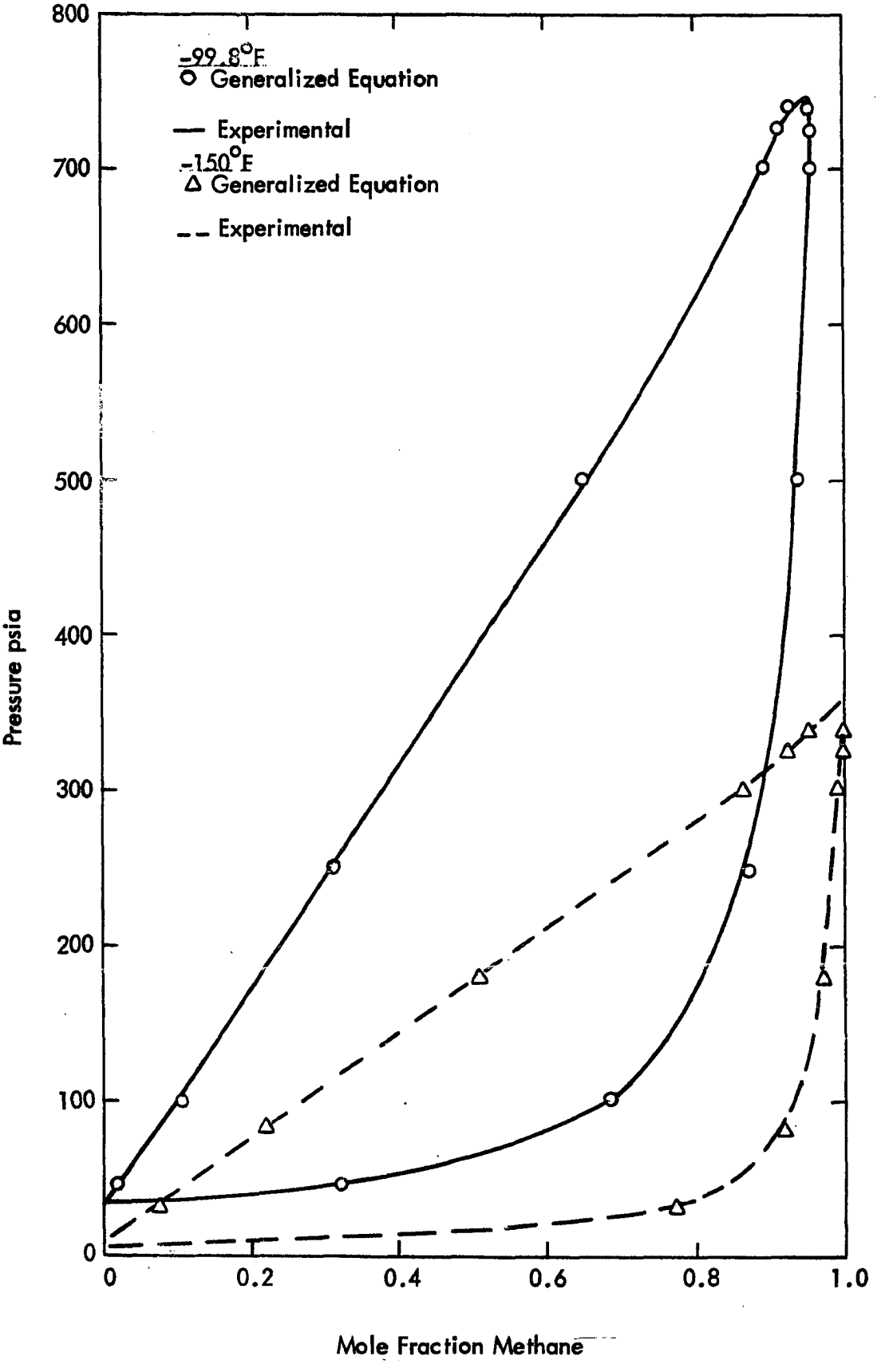

Figure VI-8 Comparison of Predicted and Experimental Phase Compositions for the Methane-Ethane System at -99.8° and -150°F.

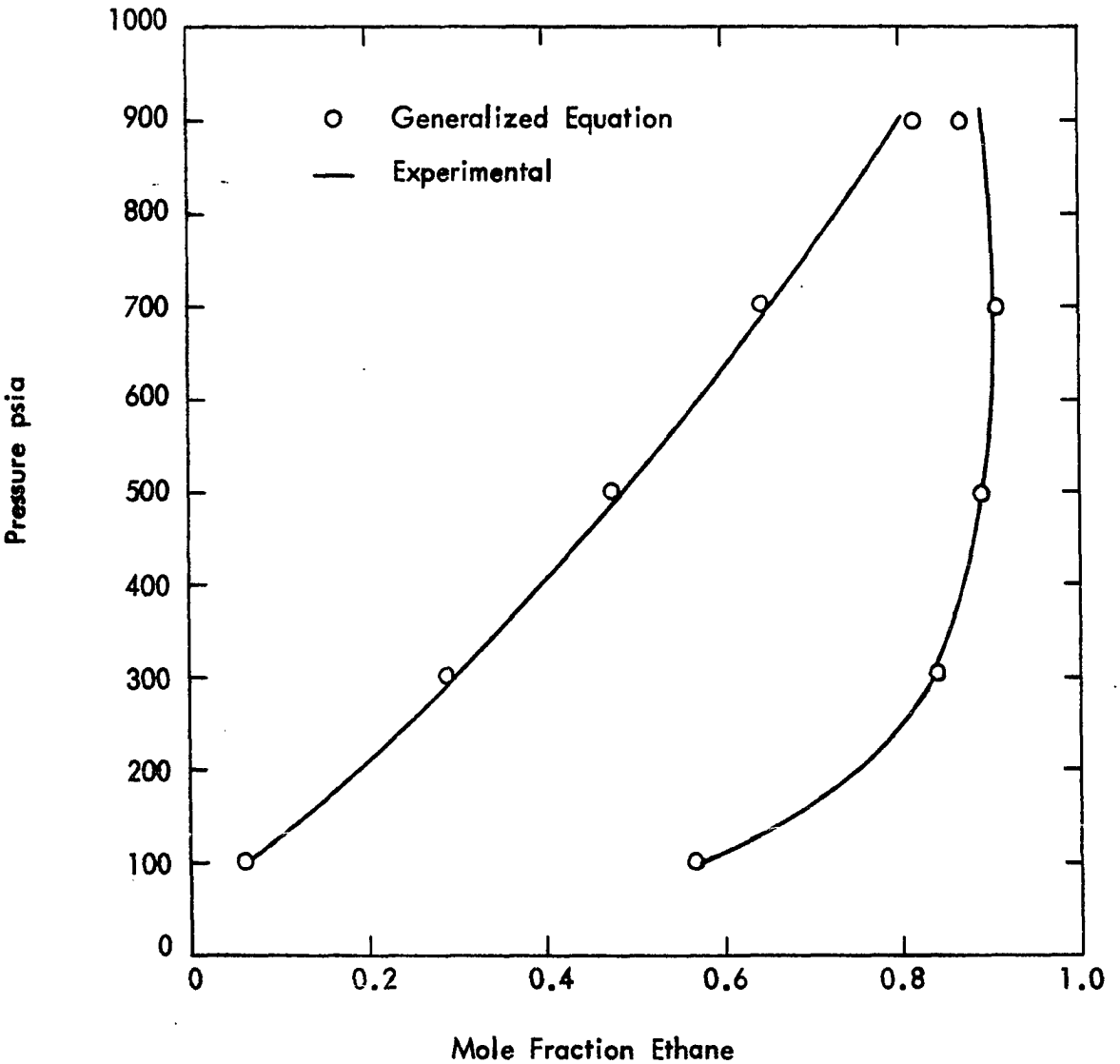

Figure VI-9 Comparison of Predicted and Experimental Phase Compositions for the Ethane-n-Pentane System at 160°F.

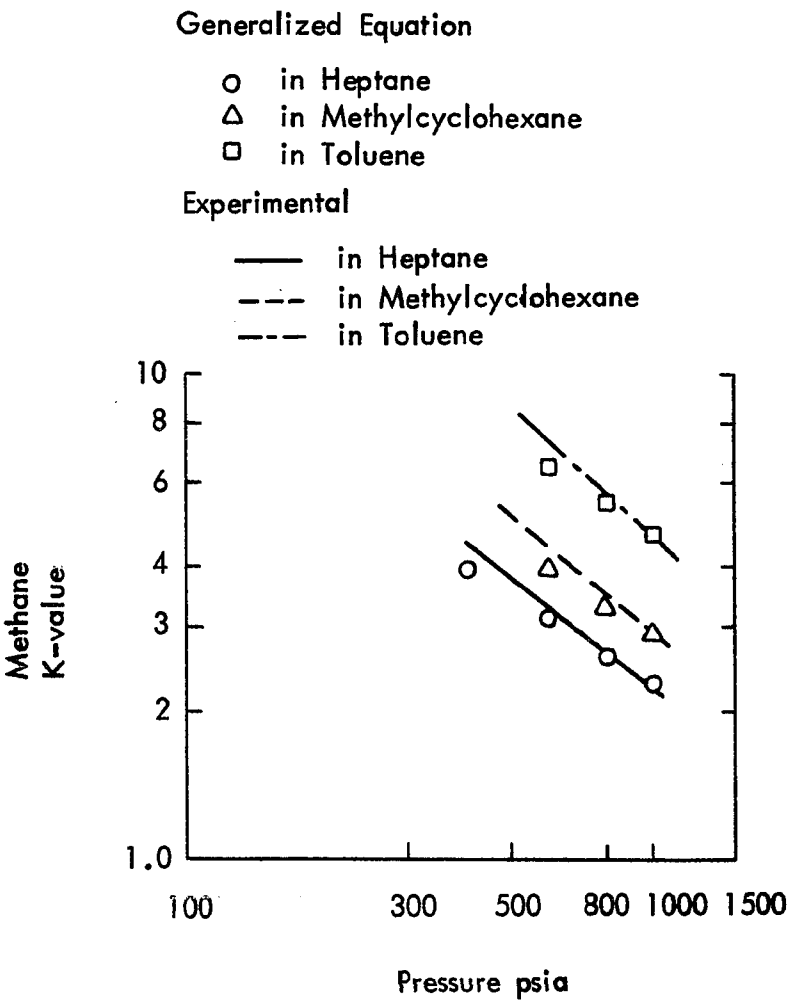

Figure VI-10 Comparison of Predicted and Experimental Methane K-values for the Methane-Heptane, Methane-Toluene & Methane-Methylcyclohexane Systems at -40°F.

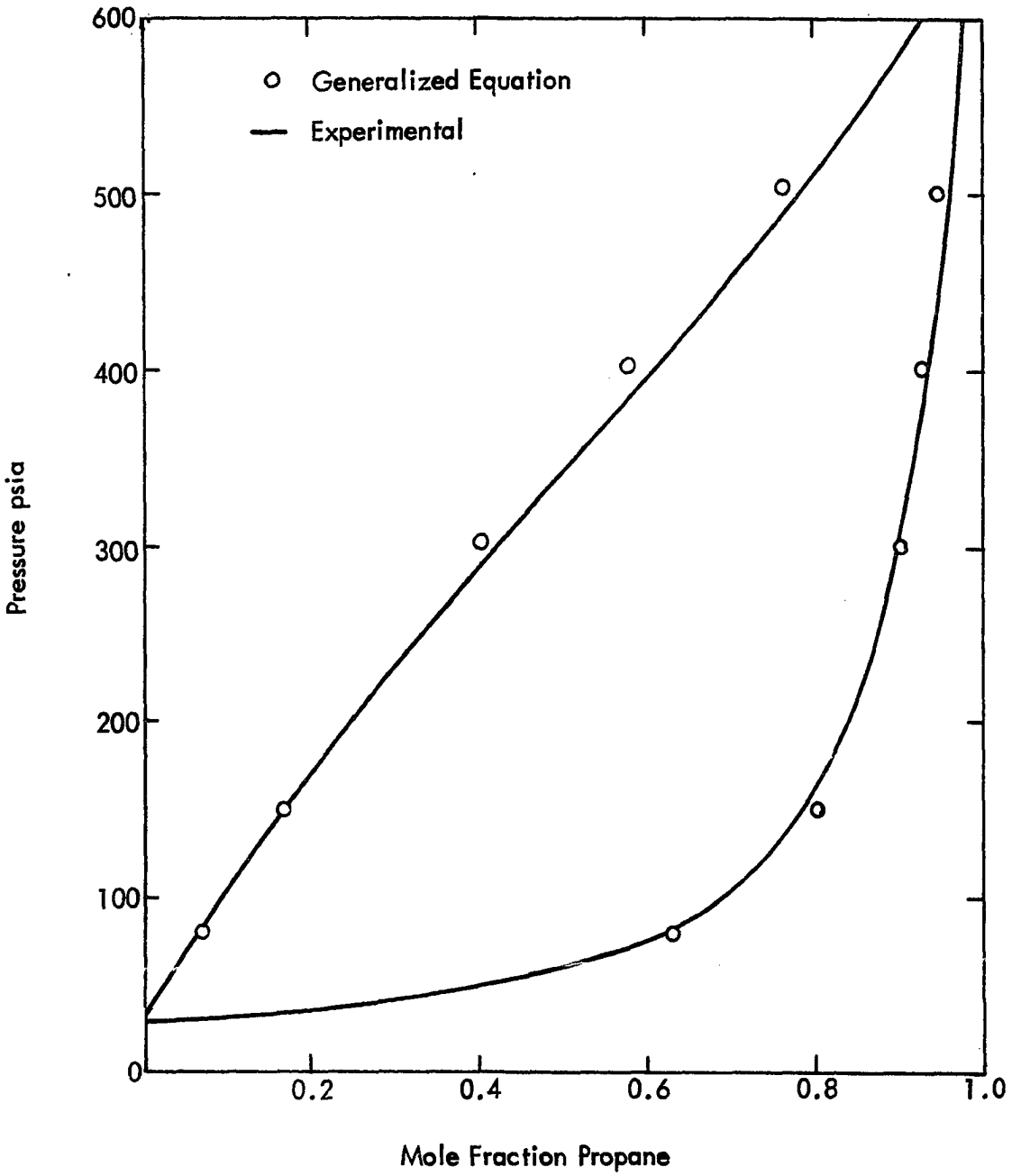

Figure VI-11 Comparison of Predicted and Experimental Phase Compositions for the Propane-Benzene System at 220°F.

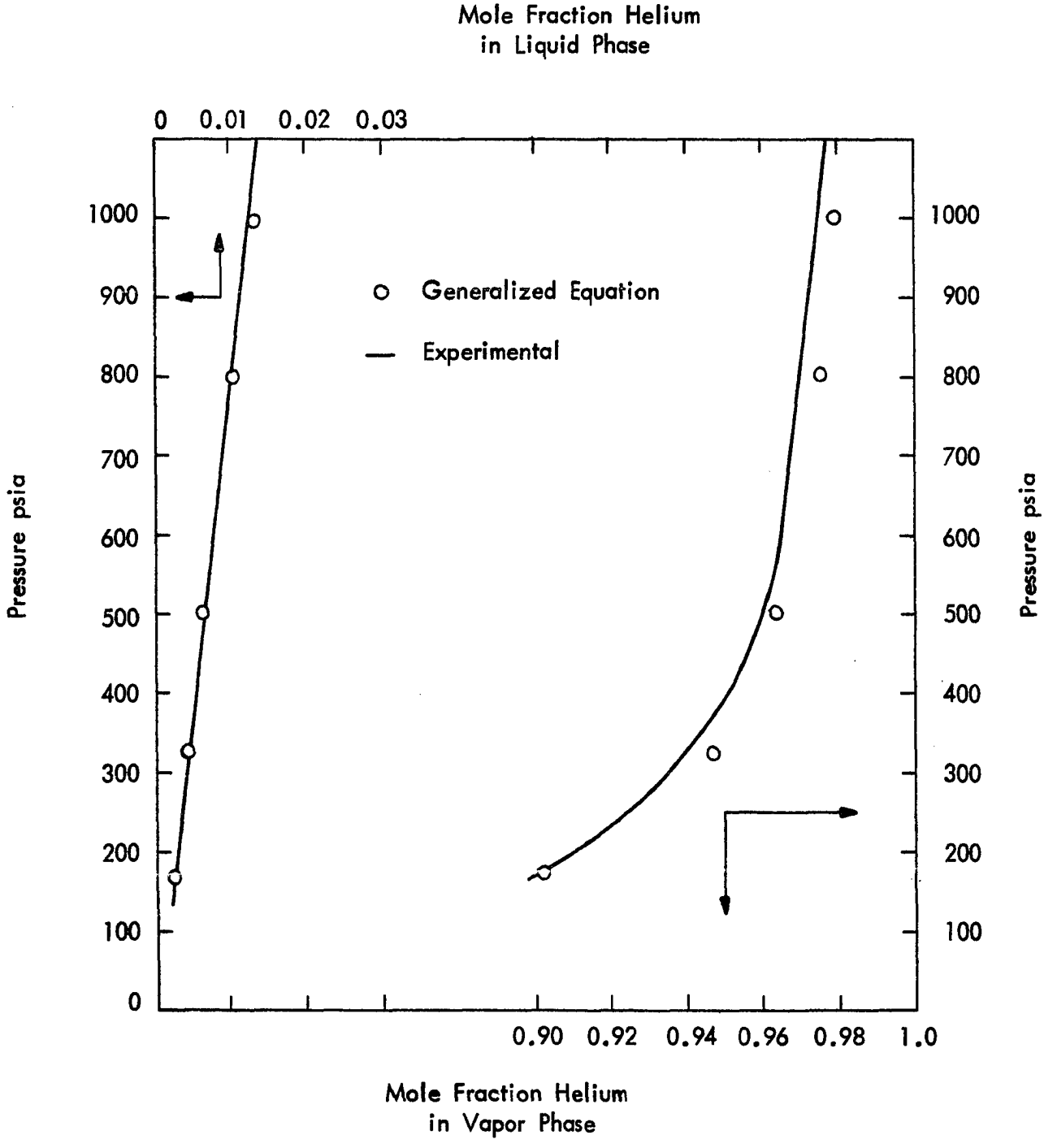

Figure VI-12 Comparison of Predicted and Experimental Phase Compositions for the Helium-Nitrogen System at -320.7°F.

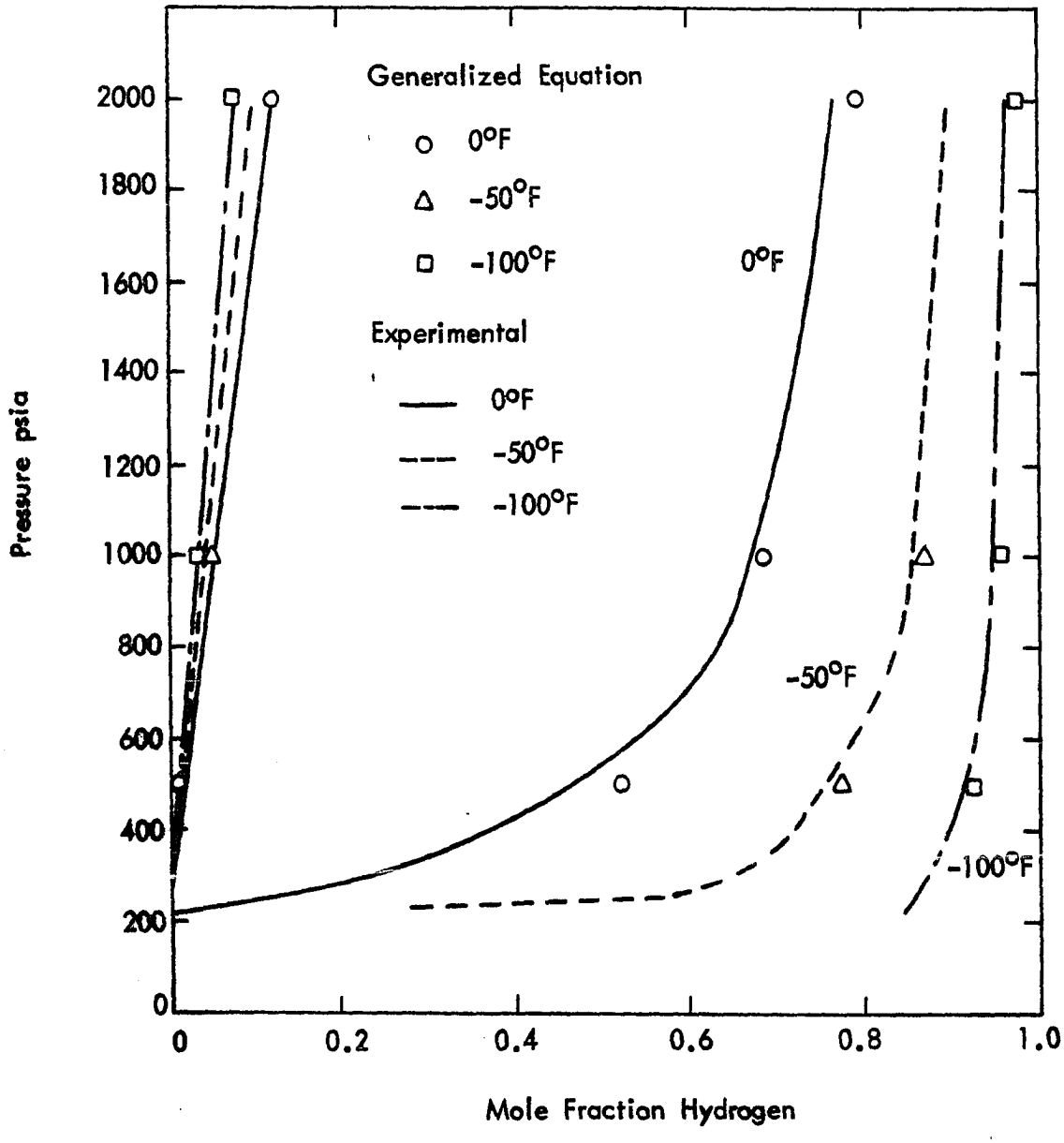

Figure VI-13 Comparison of Predicted and Experimental Phase Compositions for Hydrogen-Ethane System at -100°F, -50°F and 0°F.

CHAPTER VII

INDUSTRIAL APPLICATIONS OF THE GENERALIZED CORRELATION

The generalized equation of state correlation can be used for many practical calculations encountered in the hydrocarbon processing industry. A number of these industrial applications of the correlation are discussed here to demonstrate the practical value of the correlation through direct comparisons of predicted and experimental data. The presentation for each process discusses important features of the process for which calculations can be made effectively using the generalized correlation.

Nitrogen separation from natural gas by conventional low temperature flash and distillation methods generally involves processing of mixtures which are principally nitrogen and methane. For example, in helium recovery processes, the major constituents of the mixtures involved are methane and nitrogen over a wide range of the temperatures involved in the process. Thus, for design calculations for nitrogen separation from natural gas, the ability to accurately predict enthalpies and K-values for the methane-nitrogen system is quite important. The enthalpy of the methane-nitrogen system is predicted within 1.03 Btu/lb of the experimental data, down to -250°F. Vapor and liquid compositions in Figure (VI-2) are in close agreement with experimental data at 300 and 500 psia down to -240°F. Thus, the generalized equation of state obviously is

suitable for design of processes for nitrogen separation from natural gas and related processes involving mixtures whose major constituents are methane and nitrogen.

Helium-nitrogen separation by low temperature flash methods require high purity helium in the vapor phase and small loss of helium in the liquid phase in the final separation step. Vapor-liquid equilibrium data for the helium-nitrogen system obtained by Buzyna[12] at temperatures from -320.7°F to -238.6°F indicate that high concentrations of helium in the vapor phase can be obtained only at the lower temperatures. For this reason, only the data of Buzyna[12] at -320.7°F were used for determination of the value of the interaction parameter, $k_{ij} = 0.24$. The characterization parameters used for helium are $\omega = 0$, $\rho_c = 1.0861$ lb-moles/cu. ft. and $T_c = -450.33°F$. A plot of predicted vapor and liquid compositions is shown in Figure VI-12 for -320.7°F at pressures from 328 psia to 1000 psia. The predicted phase compositions are in good agreement with experimental data at -320.7°F. For temperatures above -320.7°F, there is reduction in the accuracy of vapor-liquid equilibrium predictions, although bulk property predictions should be adequate for engineering calculations.

Processing of systems containing hydrogen poses many problems from the standpoint of thermodynamic predictions. No correlation has yet been capable of totally general predictions of the behavior of systems containing hydrogen. To describe gas mixtures, Prausnitz and Gunn[81] utilized critical constants for hydrogen differing from the true critical constants. A similar approach has proved feasible in the present correlation. Characterization parameters used here for hydrogen are $\omega = 0$ and $\rho_c = 1.2486$ lb-moles/cu. ft. at all conditions and $T_c = -375.°F$ ($T \geq 0°F$), $T_c = -395°F$ ($0°F > T >$

$-100^{o}F$), and $T_c = -410^{o}F$ ($-100^{o}F \geq T$). With the use of these characterization parameters, predicted densities for hydrogen-methane and hydrogen-ethane mixtures agree with the experimental data of Solbrig[95] with average absolute deviations of 1.5% and 2.0%, respectively. Vapor-liquid equilibrium predictions for the hydrogen-ethane system at $-100^{o}F$, $-50^{o}F$ and $0^{o}F$ are predicted with good accuracy, as shown in Figure VI-13. The values of k_{ij} used in these calculations were $k_{ij} = 0.01$ for hydrogen-methane and $k_{ij} = 0.02$ for hydrogen-ethane. Phase compositions for the hydrogen-methane-ethane system are also accurate, Table VI-8.

Hydrogen sulfide-hydrocarbon system process calculations can be made using the generalized correlation. Comparison calculations for vapor-liquid equilibrium show good accuracy of predictions for methane-hydrogen sulfide and propane-hydrogen sulfide systems, Figures VI-3 and VI-5. Also, comparisons with methane-hydrogen sulfide density data indicate that densities of natural gases containing even large amounts of hydrogen sulfide should be predicted accurately.

Carbon dioxide-hydrocarbon system calculations also can be made using the correlation. As shown in Figure VI-4, quite accurate K-values are obtained for the propane-carbon dioxide system. In addition, carbon dioxide K-values even in fifteen component absorber systems are predicted with the accuracy required for engineering design calculations, as shown in Table VI-10.

LNG processing requires the calculation of densities, enthalpies and vapor-liquid equilibrium of the LNG (liquefied natural gas). The densities of three simulated LNG mixtures are predicted within 1% of the experimental data, for which the reported uncertainty is 1%. The enthalpy of the natural gas mixture discussed previously is predicted within 2 Btu/lb of experimental

enthalpies, for which the probable uncertainty is roughly 2 Btu/lb. The vapor and liquid compositions of the natural gas mixture in Table VI-9 are predicted within roughly two to three times the experimental uncertainty, with the predicted K-values of the major constituent of natural gas, methane, differing from the experimental value by less than 2% at -120°F and -195.0°F. It should be noted that LNG mixture data are generally less accurate than most of the binary and ternary data for the lighter systems. Therefore, these LNG property predictions must be considered quite adequate for LNG processing calculations.

Natural gas liquefaction using mixed refrigerants requires accurate prediction of mixed refrigerant enthalpy and K-values. Some of the mixtures studied have compositions and characteristics approaching mixed refrigerants. The enthalpy of the methane-ethane-propane system is predicted within 1.74 Btu/lb of experimental data, indicating the generalized correlation can be used for mixed refrigerant enthalpy calculations. Vapor and liquid compositions for the methane-ethane-propane system in Table IV-5 generally are predicted within 5% or 0.0005 mole fraction, whichever is larger, indicating the correlation can be used successfully for mixed refrigerant vapor-liquid equilibrium calculations.

Cryogenic processing of natural gas by turbine expansion requires the accurate prediction of natural gas entropy from the high temperature, high pressure gas phase to the low temperature, moderate pressure two-phase region. Use of the generalized technique to predict the entropy of natural gas and LNG was tested using entropy values for a nominal 94.8 mole percent methane and 5.2 mole percent propane mixture. For the temperature range from -250 to +300°F and pressure range from 250 to 2000 psia, entropies are predicted with an uncertainty of only 0.0042 Btu/lb-°F. These results indicate the

generalized correlation can be used with confidence for entropy calculations in cryogenic processing design.

Low temperature separations of light hydrocarbons require accurate predictions of enthalpies and K-values for system types exampled by a number of the mixtures studied. When lower processing temperatures are reached, very little butane or heavier components remain in process streams. Thus, the various mixtures of methane, ethane and propane are useful for evaluating the generalized correlation for low temperature hydrocarbon separation calculations. For the several mixtures of methane, ethane or propane, predicted enthalpies generally are within 2 to 4 Btu/lb of experimental data, which is adequate for most process calculations. For the binary and ternary systems composed of methane, ethane or propane, predicted vapor and liquid compositions are within the larger of 5% or 0.0005 of the experimental mole fraction at most points. Direct comparisons with experimental data are given in Figures VI-6, VI-7 and VI-8 and Table VI-5.

Low temperature processing using absorbers requires accurate enthalpies and K-values for the complex multicomponent systems encountered in this type of processing. The NGPA absorber system vapor-liquid equilibrium data[114] for a 103 molecular weight (MW) lean oil were used in testing the generalized correlation. The information reported for the lean oil heavier fractions consisted of boiling range, average molecular weight, density and lean oil P-N-A (paraffin-naphthene-aromatic) analysis. The following correlation for the critical temperature, critical density and acentric factor of lean oil fractions was used,

$$T_c = (P + F_1 N + G_1 A)\ T_{cp} \qquad \text{(VII-1)}$$

$$\rho_c = (P + F_2 N + G_2 A)\, \rho_{cp} \qquad \text{(VII-2)}$$

$$\omega = (P + F_3 N + G_3 A)\, \omega_p \qquad \text{(VII-3)}$$

In these relations T_{cp}, ρ_{cp}, and ω_p are the critical temperature, critical density and acentric factor of the normal paraffin having the same carbon number as the lean oil fraction. P, N and A are the mole fractions of paraffins, napthenes and aromatics in the lean oil. F_1, F_2 and F_3, respectively, are constants defined as the ratios of cyclohexane to n-hexane critical temperatures, critical densities, and acentric factors. G_1, G_2 and G_3 are defined similarly as the ratios of benzene to n-hexane characterization parameters. Calculations using these characterization parameters, yield absorber system vapor and liquid compositions which are in good agreement with the experimental data. In addition, the enthalpy for a rich absorber oil mixture is predicted within 3.3 Btu/lb of experimental data[115] in the range from -100°F to 600°F and 50 psia to 2500 psia. These studies indicate the generalized correlation can be utilized for low temperature absorber calculations.

Processing of light naphthas requires accurate information regarding the properties of the naphthas. Lenoir and Hipkin[62] recently have measured the enthalpy of a light naphtha in the temperature range from 300°F to 600°F at pressures up to 1400 psia. Comparison calculations at eighteen data points show the generalized equation of state correlation predicts the enthalpy of this light naphtha with an average absolute deviation of 1.6 Btu/lb, which approaches the reported experimental uncertainty of 1.5 Btu/lb. In performing these calculations, the reported characteristics of the light naphtha heavier fractions were used to determine an equivalent P-N-A analysis, allowing the methods discussed for calculating lean oil fraction characterization parameters to be used for the naphtha heavier fractions.

The processing situations discussed above by no means exhausts the list of potential industrial applications of the generalized correlation presented here. The discussion does demonstrate clearly that the correlation can be used for widely varying systems and processing conditions.

CHAPTER VIII

CONCLUSIONS

It is obvious from the many comparison tests which have been made, that the generalized equation of state correlation presented here accurately predicts densities, enthalpies, entropies and vapor-liquid equilibria of mixtures as well as pure fluids.

Use of multiproperty regression analysis in determining the generalized parameters has ensured the thermodynamic consistency of the correlation. Because of the thermodynamic consistency of the generalized correlation, other bulk properties such as heat capacities, Joule-Thomson coefficients, etc., not utilized in the regression calculations, can be calculated with confidence of accuracy. No previous generalized correlation has been capable of accurate and self consistent predictions of all thermodynamic properties and vapor-liquid equilibria for such wide classes of fluids over such broad ranges of conditions.

From the standpoint of use for industrial calculations, a very important feature of the generalized correlation is the nature of its generality. Only the pure fluid characteristics critical temperature, critical density and acentric factor, and interaction parameters for binary pairs are required for prediction calculations of fluid thermodynamic behavior. Values of the acentric factor reported in the literature yield good accuracy for most fluids. If greater accuracy of predictions is desired,

the characterization factor ω for use in the generalized correlation can be determined from vapor pressure data using the technique described in Chapter II.

Predictions of thermodynamic behavior in the regions between $T_r = 0.83$ and $T_r = 1.0$, including prediction of the critical point, are very accurate using values for the reduced parameters B_o', b' and c' determined from critical constraints. Generation of the values of B_o', b' and c' for use in the critical region involves simply solving the three simultaneous critical constraint equations.

Parameter mixing rules which utilize the interaction parameter k_{ij} in characterizing terms corrrsponding to the second virial coefficient (A_o, C_o, D_o and E_o) have been used in this work. These mixing rules have been found to be of greater practical value for industrial applications than the rules used by Bishnoi and Robinson[8] for the BWR equation, which include k_{ij} in characterizing terms corresponding to the third virial coefficient. Use of k_{ij} in only second virial coefficient terms shortens vapor-liquid equilibrium computing time significantly compared to using k_{ij} also in third virial coefficient terms and in addition, yields more accurate predictions for the correlation used here.

Development of a versatile and industrially practical computer program using the new generalized correlation is feasible because one calculation procedure accurately predicts fluid thermodynamic properties and phase equilibria for any mixture or pure compound.

REFERENCES

1. Akers, W. W., L. L. Attwell and J. A. Robinson, Ind. Eng. Chem., 46, 2536 (1954).

2. Akers, W. W., R. E. Kelly and T. G. Lipscomb, Ind. Eng. Chem., 46, 2535 (1954).

3. Aston, J. G. and S. C. Schumann, J. Am. Chem. Soc., 64, 1034 (1942).

4. Benedict, M., G. B. Webb, and L. C. Rubin, J. Chem. Phys., 8, 334 (1940).

5. Benedict, M., G. B. Webb, and L. C. Rubin, J. Chem. Phys., 10, 747 (1942).

6. Bhirud, V. L. and J. E. Powers, "Thermodynamic Properties of a 5 Mole Percent Propane in Methane Mixture," Report to the Natural Gas Processors Association, Tulsa, Oklahoma, August, 1969.

7. Bierlein, J. A., W. B. Kay, Ind. Eng. Chem., 45, 619 (1953).

8. Bishnoi, P. R. and D. B. Robinson, Can. J. Chem. Eng., 50, 101 (1972).

9. Bloomer, O. T., D. C. Gami, J. D. Parent, Inst. Gas Tech. Res. Bull., 22, (1953).

10. Bono, J. L., and K. E. Starling, Can. J. Chem. Eng., 48, 468 (1970).

11. Brewer, J., N. Rodewald, F. Kurata, A.I.Ch.E. J., 7, 13 (1961).

12. Buzyna, G., M. S. thesis, Illinois Institute of Technology (1962).

13. Canjar, L. N., R. F. Smith, E. Volianitis, J. F. Galluzzo, and M. Cabarcos, Ind. Eng. Chem., 47, No. 5, 1028 (1955).

14. Canjar, L. N., and F. S. Manning, Thermodynamic Properties and Reduced Correlations for Gases, Gulf Publishing Company, Houston (1967).

15. Chang, H. L. and R. Kobayashi, J. Chem. Eng. Data, 12, 520 (1967).

16. Chang, H. L. and R. Kobayashi, J. Chem. Eng. Data, 12, 517 (1967).

17. Chang, H. L., R. Kobayashi, and L. J. Hurt, J. Chem. Eng. Data, 12, 1212 (1967).

18. Clements, L. D., J. H. Christensen and K. E. Starling, Proceedings of of the Oklahoma Academy of Science, 51, (1971).

19. Cosway, H. F. and D. L. Katz, A.I.Ch.E. J., 5, 46 (1959).

20. Couch, E. J., L. J. Hirth, and K. A. Kobe, J. Chem. Engr. Data., 6, 229 (1961).

21. Cox, K. W., J. L. Bono, Y. C. Kwok and K. E. Starling, "Multiproperty Analysis Modified BWR Equation for Methane from PVT and Enthalpy Data," I&EC Fundamentals, 10, 245 (1971).

22. Curl, R. F. Jr., and K. S. Pitzer, Ind. Eng. Chem., 50, No. 2, 265 (1958).

23. Depriester, C. L., Chem. Eng. Pro. Symp. Ser., 49, (1953).

24. Din, F., Thermodynamic Functions of Gases, 1, Butterworths, London (1961).

25. Donnelly, H. G. and D. L. Katz, Ind. Eng. Chem., 46, 511 (1954).

26. Douslin, D. R., R. H. Harrison, R. T. Moore, and J. P. McCullough, J. Chem. Eng. Data, 9, 358 (1964).

27. Eakin, B. E., R. T. Ellington and D. C. Gami, Inst. Gas Tech. Res. Bull., 26 (1955).

28. Edminster, W. C., J. Vairogs, and A. J. Klekers, A.I.Ch.E. J., 14, No. 3, 479 (1968).

29. Farrington, P. S. and B. H. Sage, Ind. Eng. Chem., 41, No. 8, 1734 (1949).

30. Felsing, W. A., and G. M. Watson, J. Am. Chem. Soc., 64, 1822 (1942).

31. Fisher, G. D. and T. W. Leland, Jr., "The Corresponding States Principle Using Shape Factors," paper presented at 159th ACS Meeting, Houston, 1970.

32. Fisher, G. D. and T. W. Leland, Jr., Proceedings of the Natural Gas Processors 48th Annual Convention, 57 (1969).

33. Friedman, A. S., and White, D., J. Am. Chem. Soc., 72, 3931 (1950).

34. Furtado, A. W., D. L. Katz and J. E. Powers, paper presented at 159th National ACS Meeting, Houston, Feb., 1970.

35. Gilliland, E. R., and M. D. Parekh, Ind. Chem. Eng., 34, No. 3, 360 (1942).

36. Gregory, D. P., L. Djordjevich, R. Kao, G. L. Anderson, B. E. Eakin, W. W. Bodle and K. E. Starling, Project BR-4-8 Final Report, Institute of Gas Technology, June, 1971.

37. Hanson, G. H. and G. G. Brown, Ind. Eng. Chem., 37, 821 (1945).

38. Hougen, O. A., K. M. Watson and R. A. Ragatz, Chemical Process Principles, Part II, John Wiley and Sons, Inc., New York (1962).

39. Hsu, C. C. and J. J. Mcketta, J. Chem. Eng. Data, 9, 45 (1964).

40. Huang, E. T. S., G. W. Swift, and F. Kurata, A.I.Ch.E.J., 12, 932 (1966).

41. Huang, E. T. S., G. W. Swift and F. Kurata, A.I.Ch.E.J., 13, 189 (1967).

42. Johnson, D. W. and C. P. Colver, "A Method for Predicting Mixture Enthalpy Departures," paper presented at 49th Natural Gas Processors Annual Convention, Denver, 1970.

43. Johnson, D. W., and C. P. Colver, Hydrocarbon Processing, 47, 79 (1968).

44. Jones, M. L., Jr., Ph.D. Thesis, University of Michigan (1961).

45. Kang, T. L., L. J. Hirth, K. A. Kobe and J. J. Mcketta, J. Chem. Eng. Data, 6, 220 (1961).

46. Kaufmann, T. G., Ind. Eng. Chem. Fundamentals, 7, No. 1, 115 (1968).

47. Kay, W. B., Ind. Eng. Chem., 30, No. 4, 459 (1938).

48. Kay, W. B., and G. M. Rambosek, Ind. Eng. Chem., 45, No. 1, 221 (1953).

49. Kay, W. B., Ind. Eng. Chem., 33, 590 (1941).

50. Kohn, J. P., F. Kurata, A.I.Ch.E. J., 4, 211 (1958).

51. Kohn, J. P., A.I.Ch.E. J., 7, 514 (1961).

52. Kohn, J. P., J. Chem. and Eng. Data, 9, 5 (1964).

53. Kohn, J. P., J. Chem. and Eng. Data, 7, 33 (1962).

54. Kurata, F. and R. H. Jensen, J. Pet. Tech., 683 (June 1969).

55. Kurata, F. and G. W. Swift, Report to Natural Gas Processors Association, RR-5, Dec., (1971).

56. Kwok, Y. C., and K. E. Starling, Advances in Cryogenic Engineering, 16, 54 (1971).

57. Kwok, Y. C., J. E. Powers and K. E. Starling, Proceedings of the Oklahoma Academy of Science, 51, (1971).

58. Lapidus, L., Digital Computation for Chemical Engineers, McGraw-Hill, New York, (1962).

59. Lenoir, J. M., G. K. Kuravila and H. G. Hipkin, paper presented at 34th Midyear Meeting of API Division of Refining, Philadelphia, May, 1969.

60. Lenoir, J. M., D. R. Robinson and H. G. Hipkin, Preprint No. 20-68, 33rd Midyear Meetings, API Division of Refining, Philadelphia, May, 1968.

61. Lenoir, J. M., private communication.

62. Lenoir, J. M. and H. G. Hipkin, Hydrocarbon Processing, 5, 95 (1971).

63. Lewis, L. C., and W. J. Fredericks, J. Chem. Eng. Data, 13, No. 4, 482 (1968).

64. Lin, C. J., Y. C. Kwok and K. E. Starling, "Modified BWR Equation for the Methane-Propane System from Multiproperty Analysis of PVT, Enthalpy, Vapor Pressure and Vapor-Liquid Equilibrium Data," to appear in Can. J. Chem. Eng.

65. Lin, C. J., Y. C. Kwok and K. E. Starling, Can. J. Chem. Eng. (to appear).

66. Mage, D. T., M. C. Jones, Jr., D. L. Katz, and J. R. Roebuck, Chem. Eng. Prog. Sym. Series, 59, No. 44, 61 (1963).

67. Manker, E. A., Ph.D. Thesis, University of Michigan (1964).

68. Mather, A. E., Ph.D. Thesis, University of Michigan (1967).

69. Matheson Gas Data Book, 4th ed., The Matheson Co., East Rutherford, N.J., 1966.

70. Mathews, C. S., and C. O. Hurd, Trans. A.I.Ch.E., 42, 55 (1946).

71. Mehra, V. S. and G. Thodos, J. Chem. Eng. Data., 10, 211 (1965).

72. Michels, A., J. de Gryter, and F. Niesen, Physica, 3, 347 (1936).

73. Michels, A., T. Wassenaar, P. Louwerse, R. J. Lunbeck, and G. P. Walkers, Physica, 19, 287 (1953).

74. Mundel, C. F., Z. Phys. Chem., 85, 435 (1913).

75. Opfell, J., W. G. Schlinger and B. H. Sage, Ind. Engr. Chem., 46, 189 (1954).

76. Organick, E. I. and W. R. Studhalter, Chem. Eng. Prog., 44, 847 (1940).

77. Petroleum Processing Handbook, McGraw-Hill Book Co., New York, 1967.

78. Powers, J. E. private communication.

79. Powers, J. E., E. A. Manker, A. E. Mather and V. F. Yesavage, paper presented at A.I.Ch.E. 65th National Meeting, March 4-7, 1969, Cleveland.

80. Prausnitz, J. M. and Chueh, P. L., Computer Calculations for High-Pressure Vapor-Liquid Equilibria, Prentice-Hall, 1968.

81. Prausnitz, J. M. and R. D. Gunn, A.I.Ch.E. Journal, 4, 430 (1958).

82. Reamer, H. H., B. H. Sage, and W. N. Lacey, Ind. Eng. Chem., 42, No. 1, 140 (1950).

83. Reamer, H. H., B. H. Sage, W. N. Lacey, Ind. Eng. Chem., 43, 976 (1951).

84. Reamer, H. H., B. H. Sage, W. N. Lacey, Ind. Eng. Chem., 43, 2515 (1951).

85. Reamer, H. H. and B. H. Sage, J. Chem. Eng. Data, 7, 161 (1962).

86. Reamer, H. H., J. Chem. Eng. Data, 5, 44 (1960).

87. Reamer, H. H. and B. H. Sage, J. Chem. Eng. Data, 9, 24 (1964).

88. Reamer, H. H. and B. H. Sage, J. Chem. Eng. Data, 11, 17 (1966).

89. Redlich, O., and J. N. S. Kwong, Chem. Rev., 44, 233 (1949).

90. Rossini, F. D., et al., API Research Project 44, Carnegie Press, Pittsburgh (1953).

91. Sage, B. H., and W. N. Lacey, Thermodynamic Properties of the Lighter Paraffin Hydrocarbons and Nitrogen, A.P.I., New York (1950).

92. Sage, B. H. and W. N. Lacey, Ind. Eng. Chem., 32, 992 (1940).

93. Sage, B. H. and W. N. Lacey, Some Properties of the Lighter Hydrocarbons, Hydrogen Sulfide, and Carbon Dioxide, API., New York (1955).

94. Silberberg, H., McKetta, J. J. and Kobe, K. A., J. Chem. Eng. Data, 4, 323 (1959).

95. Solbrig, C. W., M.S. thesis, Illinois Institute of Technology (1962).

96. Starling, K. E. and J. F. Wolfe, Proceedings of the Oklahoma Academy of Science, 51 (1971).

97. Starling, K. E., "Applications of Multiproperty Analysis in Equation of State Development and Thermodynamic Property Prediction," Proceedings of the Natural Gas Processors Association, 49 (1970).

98. Starling, K. E., "Thermo Data Refined for LPG," Hydrocarbon Processing, 3, 101 (1971).

99. Starling, K. E. and Powers, J. E., "Enthalpy of Mixtures by Modified BWR Equation," I&EC Fundamentals, 9, 531 (1970).

100. Starling, K. E., "New Method for Determining Equation of State Parameters from Phase Equilibria Data," Soc. Pet. Engr. J., 363, Dec. (1966).

101. Stewart, D. E., B. H. Sage, and W. N. Lacey, Ind. Eng. Chem., 46, No. 12, 2529 (1954).

102. Streett, W. B. and L. A. K. Staveley, Advances in Cryogenic Engineering, 13, 363 (1968).

103. Stuart, E. B., K. T. Yu, and J. Coull, Chem. Eng. Prog., 46, No. 6, 311 (1950).

104. Su, G. J. and D. S. Viswanath, A.I.Ch.E. J., 11, 205 (1965).

105. Tickner, A. W. and F. P. Lossing, J. Phys. Colloid Chem., 55, 733 (1951).

106. Vairogs, J., A. J. Klekers and W. C. Edmister, A.I.Ch.E. J., 17, 308 (1971).

107. Van Horn, L. D., Ph.D. thesis, Rice University (1966).

108. Van Itterbeek, A., O. Verbeke, and K. Staes, Physica, 29, No. 6, 742 (1963).

109. Vennix, A. J., Ph.D. Thesis, Rice University (1967).

110. Walters, C. J. and J. M. Smith, Chem. Eng. Prog., 48, 342 (1952).

111. West, J. R., Chem. Eng. Prog., 44, No. 4, 287 (1948).

112. Wichterle, I. and R. Kobayashi, Monograph, Rice University (1970).

113. Williams, R. B. and D. L. Katz, I.E.C. Eng. Design and Process Development, 46, 2512 (1954).

114. Wilson, G. M., S. T. Barton and H. J. Tullos, "K-values in Absorber Oil-Natural Gas Systems, Experimental Study," Report for Natural Gas Processors Association, Sept. 5, 1968.

115. Wilson, G. M., B. E. Eakin, W. E. DeVaney and S. T. Barton, Interim Progress Report to Natural Gas Processors Association, July, 1971.

116. Yesavage, V. F., Ph.D. Thesis, University of Michigan (1968).

117. Zenner, G. H. and L. I. Dana, Chem. Eng. Prog. Symp. Ser., 59, 36 (1963).

118. Zudkevitch, D. and J. Joffe, A.I.Ch.E. J., 16, 112 (1970).

NOMENCLATURE

A and B	generalized equation of state parameters
$B_o, A_o, C_o, D_o, E_o, b, a, c, d, \alpha, \gamma$	equation of state parameters
$B'_o, A'_o, C'_o, D'_o, E'_o, b', a', c', d', \alpha', \gamma'$	reduced equation of state parameters
F	function minimized in vapor-liquid equilibrium predictions
$F_1, F_2, F_3, G_1, G_2, G_3$	heavy oil fraction characterization correlation parameters
FN(i)	calculated pressure using Equation II-1 for the density value at i^{th} iteration minus the given pressure
f	fugacity
$\bar{f}_i$	fugacity of i^{th} component in a mixture
H	enthalpy, Btu/lb
$(H-H^o)$	enthalpy for the real gas less the enthalpy for the ideal gas at the same temperature, Btu/lb
H^o	enthalpy of ideal gas, Btu/lb
K_i	K-value for i^{th} component
k_{ij}	interaction parameter for i^{th} and j^{th} components
L	moles of liquid per mole of feed
M	molecular weight
MD	density key

NC	number of pure components
$(NP)_i$	number of data points of the i^{th} component for each property
n	total number of components
n_i	number of moles of i^{th} component in a mixture
P	absolute pressure, psia
P,N,A	mole fractions of paraffins, naphthenes and aromatics in a mixture
P_c	critical pressure, psia
Q	function to be minimized in the multiproperty regression calculation
R	gas constant
R_i	estimate of K-value for i^{th} component
S	entropy, Btu/lb.^oR
$(S-S^o)$	entropy for the real gas less the entropy for the ideal gas at the same temperate, Btu/lb.^oR
S^o	entropy of ideal gas at unit pressure, Btu/lb.^oR
T	temperature, ^oR
T_c	critical temperature, ^oR
V	volume of phase, also moles of vapor per mole of feed
x_i	mole fraction of i^{th} component in liquid
Y_i	mole fraction of i^{th} component in vapor
Z	compressibility factor
z_i	mole fraction of i^{th} component in feed

Greek Letters

ρ	molar density, lb-moles/cu.ft.
ρ_c	molar critical density, lb-moles/cu.ft.

Σ	summation operator
ω	acentric

Subscripts

c	critical property
i,j,k	component index or data point index
o	zt $0^{o}R$
P	paraffin
r	reduced property
s	saturated

Superscripts

L	liquid phase
V	vapor phase
o	ideal gas state
$\bar{}$	indicating partial molar quantity

Abbreviations

Abs. Dev. Avg.	absolute deviation average
Btu	British thermal unit
calc.	calculated
cu.ft.	cubic foot
% Dev	percent deviation
exp	exponential function or experimental
exptl	experimental
^{o}F	degree Fahrenheit
lb	pound
ℓn	natural logarithm function
press	pressure
psia	absolute pound-force per square inch
^{o}R	degree Rankine